

Current Distribution on Linear Thin Wire Antenna Application of MOM and FMM

Yazdan Mehdipour Attaei

Submitted to the
Institute of Graduate Studies and Research
In partial fulfillment of the requirements for the Degree of

Master of Science
in
Electrical and Electronic Engineering

Eastern Mediterranean University
February 2012
Gazimağusa, North Cyprus

Approval of the Institute of Graduate Studies and Research

Prof. Dr. Elvan Yılmaz
Director

I certify that this thesis satisfies the requirements as a thesis for the degree of Master of Science in Electrical and Electronic Engineering.

Assoc. Prof. Dr. Aykut Hocanın
Chair, Department of Electrical and Electronic
Engineering

We certify that we have read this thesis and that in our opinion it is fully adequate in scope and quality as a thesis for the degree of Master of Science in Electrical and Electronic Engineering.

Prof. Dr. Haluk U. Tosun
Supervisor

Examining Committee

1. Prof. Dr. Haluk U.Tosun

2. Prof. Dr. Osman Kükrer

3. Assist. Prof. Dr. Rasime Uygurođlu

ABSTRACT

Numerical techniques in solving electromagnetics problems are the most common methods which are used during the last decades, especially with the growing inventions of fast speed computers and powerful softwares. In this thesis, it is attempted to approach a fast efficient algorithm for solving the famous Hallen and Pocklington integral equations, regarding the current distribution on a finite-length linear thin wire antenna.

In order to approach this aim, Method of Moments (MOM) which is a powerful numerical technique to solve integral equations and Fast Multipole Method (FMM) which is a mathematical technique to accelerate iterative solutions is to be combined. Afterward, this technique will be applied on Hallen and Pocklington's integral equations (HE and PE) for a transmitting thin wire antenna which is energized by delta-function generator (DFG) in order to find current distribution along the antenna.

In the thesis, there would be a discussion part about solvability and non-solvability of HE and PE equations and comparison between the results using this technique and the ones which have been extracted by applying the other methods mentioned in different books for solving HE and PE equations in frequency domain.

Keywords: Current distribution, thin wire antenna, Hallen's integral equation, Pocklington's integral equation, Galerkin method, Entire domain basis function, Fast multipole method.

ÖZ

Bu amaçla, güçlü bir sayısal yöntem olan Moment Metodu ile ötelemeli çözümleri hızlandıran bir yöntem olan Hızlı Çok kutup Yöntemi birlikte kullanılmaktadır. Burada sayısal çözümleri yapılan Tümlev Denklemleri Hallen ve Pocklington denklemleri olarak anılmaktadır. Antenin uyarılması delta-işlevli bir kaynakla yapılmaktadır.

Bu tezde ayrıca Hallen ve Pocklington denklemlerinin çözülebilirlikleri ile ilgili bir tartışma da yer almaktadır.

Bu çalışmada elde edilen sonuçlar, başka sayısal yöntemlerle elde edilenlerle ve bazı deneysel verilerle de karşılaştırılmaktadır.

Anahtar Kelimeler: Akım dağılımı, ince tel anten, Hallen integral denklemi, Pocklington integral denklemi, Galerkin yöntemi, Tüm etki alanı bazında fonksiyonu, Hızlı çok kutuplu yöntem

To my wife, Mona

and

My parents

ACKNOWLEDGMENTS

I wish to express my deepest respect and regards to my supervisor Prof. Dr. Haluk Tosun for his unlimited supports and encouragements all along my thesis research.

I also wish to thank all the faculty members at the department of Electrical and Electronic Engineering, and specially the chairman, Assoc. Prof. Dr. Aykut Hocann.

Last but not least, I would like to thank my friend Dr. Samaneh Ghafourian for her assistance in literature edition of this thesis, and express my deepest appreciation to my family, specially my wife who without their encourage and supports, I could not be able to finalize this work.

TABLE OF CONTENTS

ABSTRACT.....	iii
ÖZ.....	iv
DEDICATION.....	v
ACKNOWLEDGMENTS.....	vi
LIST OF FIGURES.....	x
LIST OF SYMBOLS & ABBREVIATIONS.....	xii
1 INTRODUCTION.....	1
1.1 Numerical Electromagnetics.....	1
1.2 Applied Numerical Method.....	3
1.3 Optimization of the Solution.....	3
1.4 Outline.....	4
2 METHOD OF MOMENTS.....	5
2.1 Terminology.....	5
2.2 Basic Concept of MOM.....	5
2.2.1 Solving Matrix Equation.....	7
2.2.2 Classification of MOM.....	8
2.2.2.1 Basis (expansion) Functions.....	8
2.2.2.2 Weighting (testing) Functions.....	10
2.2.3 Special Terms.....	11
2.2.3.1 Method of Weighting Residuals.....	11
2.2.3.2 Galerkin's Method.....	12
2.2.3.3 Collocation Method.....	12
2.2.3.4 Least Square Method.....	12

2.3 Application on Thin Wire Antenna.....	13
2.3.1 Point Matching Method	13
2.3.1.1 Pocklington's Integral Equation	13
2.3.1.2 Hallen's Integral Equation.....	18
2.3.1.3 Moment Method Solution	19
2.3.2 Galerkin Method	25
2.3.2.1 Hallen's Integral Equation	25
2.3.2.2 Pocklington's Integral Equation	30
2.3.2.3 Moment Method Solution	30
3 Fast Multipole Method (FMM).....	33
3.1 Introduction to FMM	33
3.2 Basic Concepts.....	34
3.3 Degenerating Kernel	39
4 Application of FMM on MOM	44
4.1 Reviewing the problem.....	44
4.2 FMM and Galerkin	46
4.3 Far-field Approximation	47
4.3.1 Number of Multipoles	50
4.4 SLFMM Solution for Hallen IE.....	51
5 CONCLUSION.....	55
REFERENCES	56
APPENDICES	61
Appendix A: Matlab Programs for Point Matching MOM.....	62
A-1: Hallen's integral Equation	62
A-2: Hallen vs. Pocklington.....	63

Appendix B: Matlab Programs for Galerkin MOM.....	65
B-1: Hallen's Integral Equation ($a=L/518$)	65
B-2: Hallen's Integral Equation ($a=0.01\lambda$)	66
B-3: Pocklington's Integral Equation	67
Appendix C: Matlab Program for FMM and Galerkin Method(HE).....	69

LIST OF FIGURES

Figure 2.1: Common sub-domain basis functions	10
Figure 2.2: Uniform plane wave obliquely incident on a conducting wire.....	14
Figure 2.3: Wire Antenna with Idealized DFG.....	15
Figure 2.4: Dipole segmentation and its equivalent current	16
Figure 2.5: Geometry of the problem showing the zoning of the antenna	17
Figure 2.6: Wire antenna with N segments.....	20
Figure 2.7: Current distribution, part (a) where; $\lambda = 2(m), \ell = \lambda / 2$	22
Figure 2.8: Current distribution, part (b) where; $\lambda = 2(m), \ell = 1.5\lambda$	22
Figure 2.9: Current distribution, $\lambda = 1(m), \ell = 0.47\lambda$	24
Figure 2.10: Current distribution, Galerkin vs. Point matching (HE)	26
Figure 2.11: Current distribution (real) over the dipole.....	27
Figure 2.12: Current distribution (imaginary) over the dipole.....	28
Figure 2.13: Coefficients of the basis functions (real).....	29
Figure 2.14: Coefficients of the basis functions (imaginary)	29
Figure 2.15: Current distribution, Galerkin vs. Point matching (PE)	31
Figure 3.1: Well-separated sets	36
Figure 3.2: Grouping with respect to the target sets	36
Figure 3.3: Local expansion.....	37
Figure 3.4: Grouping with respect to the source sets	37
Figure 3.5: Far field expansion	37
Figure 3.6: Standard and single level FMM	38
Figure 3.7: MLFMM using hierarchical clustering of domain	39
Figure 3.8: Vector translation	41

Figure 4.1: Structure of the antenna with $N-1$ segments of height Δz 46

Figure 4.2: Current distribution for HE, over the thin wire, FMM..... 53

LIST OF SYMBOLS & ABBREVIATIONS

c	Speed of Light (in air)
f	Frequency
k	Wave Number
ϵ	Electrical Permittivity
η	Intrinsic Impedance
λ	Wave length
μ	Electrical Permeability
ρ	Line Current Density
ω	Angular Frequency
DFG	Delta Function Generator
EM	Electromagnetics
FMM	Fast Multipole Method
HE	Hallen's Integral Equation
IE	Integral Equation
MOM	Method of Moments
MLFMM	Multilevel Fast Multipole Method
PE	Pocklington's Integral Equation
SLFMM	Single Level Fast Multipole Method

Chapter 1

INTRODUCTION

1.1 Numerical Electromagnetics

Generally in electromagnetics, there are two ways to solve problems. One is to create a particular formulation and computational method for a specific problem when we use all terms in the instruction to simplify the solution which may even lead to a closed formula as the solution. The second method is to create general solutions which cover various types of problems, but may not be necessarily as effective as a specific solution to an especially designed problem.

Numerical solutions of integral equations, as general solutions for electromagnetic problems, are based on breaking the areas under consideration, into smaller parts with identical geometric shapes. Then, a unique formulation is applied on each of these parts and finally by rejoining them, the solution for the main problem is retrieved. Commonly in EM problems, the desired parameters which are to be found are surface or volume charge density, surface or volume current density and electromagnetic fields. The other parameters of a problem such as capacitance, input impedance, radiation pattern, losses, cut-off frequency, etc. will be derived from them.

The basic of the formulation over all of the numerical methods in EM is nothing but “Maxwell's Equations”. In each method, by using the principles of the method and

extracting appropriate mathematical relations, these equations are changed in order to be solved by numerical algorithms. In the most cases, by using the integral equations (extracted from Maxwell's Equations) and breaking the region of the integral into the smaller parts with similar geometric shapes, we change these IEs (integral equations) into the matrix equations which can be solved easily, using fast computerized algorithms.

Therefore, the first step in moment method solution in EM problems is formulating the problems in terms of integral equations. Overall, there are three types of integral equations in formulating EM problems; (1) MFIE (magnetic field integral equation), (2) EFIE (electric field integral equation) and (3) CFIE (compound field integral equation). All these equations are formulated with the help of Maxwell's equations and auxiliary potentials.

After formulating the problem, breaking the area of the object is to be performed (discretizing the related integral equation). This is so called “Meshing” operation, applicable in different ways. Choosing each way depends on the type of the formulation and geometrical shape of the object. For example, surface meshes have the shape of triangle, rectangle or multi-edge in general, if the formulation is applied on the surface of the object (like EFIE). Between the elements of surface mesh, only multi-edge and triangle are the ones which can cover the curved surfaces with a good approximation. Elements of rectangular shape have problem to approximate the double curved surfaces like the sphere and are used only for the plane-surface objects.

Apparently, numerical solutions (which is in contrast with analytical solutions) in EM problems, especially the ones in which the number of unknowns is large, brings the necessity of computer mathematical softwares and programs. In this thesis, MATLAB as a strong mathematical program will be used for calculating the desired unknowns and illustration of the correspondent figures.

1.2 Applied Numerical Method

In most of the numerical methods in electromagnetics, current or charge density will be calculated first, but sometimes the priority is by finding EM fields. For example in "Finite Element Method", first we find EM fields and then other parameters are extracted from them while in MOM, charge or current density is determined first and the rest are computed accordingly.

In chapter 2, after introducing MOM and its classifications, two particular electromagnetic problems which are Hallen's and Pocklington's integral equations will be solved for current distribution over a center-fed thin dipole antenna, using two different classes of MOM which are "Point Matching" and "Galerkin" methods and the results will be compared to each other. In addition to figures which help us in our assessments, appropriate MATLAB codes for the solutions have been provided and attached to the thesis in appendix section.

1.3 Optimization of the Solution

In order to speed up the calculation process in chapter 2, we will impose a multilevel algorithm so called "Fast Multipole Method" (FMM) to our solution. This method can accelerate the matrix-vector product as well as linear system solution which

arises from applying the Galerkin method or any similar numerical method which ends up to a matrix equation. The result of combining FMM is preserving time and memory in the computation process. In chapter 3, FMM and some of its applications will be introduced in more details.

1.4 Outline

The purpose of this thesis is to solve time harmonic HE and PE for unknown current by applying Galerkin method (which is a certain type of MOM) and to find the distribution of the current over a thin wire structure. Then we optimize our solution by performing the algorithm which is defined in FMM to reduce the computation time and the number of operations in Galerkin method from order of $N \times N$ into order of $N \log N$.

In the last chapter, Galerkin method and FMM are being combined and once more, the derived solution will be applied on the thin wire structure in order to examine its efficiency, advantages and disadvantages.

In this thesis, the considered electromagnetic structure is assumed to be a perfect conductor. Although in reality there are various types of structures in which isolating materials like dielectrics are used, analyzing EM problems in such structures requires another class of MOM and formulation which is not the subject of this thesis.

Chapter 2

METHOD OF MOMENTS

2.1 Terminology

Most solutions of functional equations can be interpreted in terms of projections onto subspaces of functional spaces. For computation, these subspaces must necessarily be finite dimensional. For theoretical work they may be infinite dimensional. The general concept of solution of equation by projection onto subspaces has a number of different names. Some of the more common ones are the method of projections, the method of weighted residuals, the Petrov-Galerkin method and the method of moments [33].

The name “Method of Moments” has been derived from the original terminology that $\int x^n f(x) dx$ is the n^{th} moment of the function $f(x)$. When x^n is replaced by an arbitrary w_n , we continue to call the integral “a moment of f ”. For the other mentioned names above, there will be brief explanations in part (2.2.3) of this thesis.

2.2 Basic Concept of MOM

The method of moments can be applied on the problems in which the formulation of them can be expressed as a linear operational equation in the form;

$$L(f) = g \tag{2.1}$$

where L in (2.1) is a linear operator. This operator can be a differential, an integral or an integro-differential operator. Here f is an unknown function and g is a known function. In the first step of MOM it is considered that f can be defined over the domain of L , (D_L) , in a linear combination form of;

$$f = \sum_{i=1}^N \alpha_i f_i \quad (2.2)$$

where α_i s are unknown scalars and f_i s are known “expansion functions” (in MOM, these expansion functions are called Basis Functions). It is necessary to mention that for approximate solutions (2.2) is a finite summation while for exact solutions, it is usually an infinite one. Using (2.1), (2.2) and linearity of L , we have;

$$\sum_{i=1}^N \alpha_i L(f_i) = g \quad (2.3)$$

Now, we define a set of linearly independent “testing functions” or “weighting functions” $\{w_1, w_2, \dots, w_N\}$ in the range of L . Taking the inner product of (2.3) with each w_j (can be considered in integral form) and using the linearity of the inner product yields;

$$\sum_{i=1}^N \alpha_i \langle w_j, L(f_i) \rangle = \langle w_j, g \rangle \quad (j = 1, 2, 3, \dots, N) \quad (2.4)$$

The above equation can be written as;

(2.5)

$$\begin{pmatrix} \langle w_1, L(f_1) \rangle & \langle w_1, L(f_2) \rangle & \cdots & \langle w_1, L(f_N) \rangle \\ \langle w_2, L(f_1) \rangle & \langle w_2, L(f_2) \rangle & \cdots & \langle w_2, L(f_N) \rangle \\ \vdots & \vdots & \ddots & \vdots \\ \langle w_N, L(f_1) \rangle & \langle w_N, L(f_2) \rangle & \cdots & \langle w_N, L(f_N) \rangle \end{pmatrix} \begin{pmatrix} \alpha_1 \\ \alpha_2 \\ \vdots \\ \alpha_N \end{pmatrix} = \begin{pmatrix} \langle w_1, g \rangle \\ \langle w_2, g \rangle \\ \vdots \\ \langle w_N, g \rangle \end{pmatrix}$$

Thus, we can write (2.5) as

$$[Z]_{N \times N} \times [I]_{N \times 1} = [V]_{N \times 1} \quad (2.6)$$

$$Z_{ij} = \langle w_j, L(f_i) \rangle \quad \text{where; } i, j = 1, 2, \dots, N$$

$$I_{i1} = \alpha_i$$

$$V_{j1} = \langle w_j, g \rangle$$

In (2.6), matrix \mathbf{Z} is usually called MOM impedance matrix while matrix \mathbf{I} contains the unknown coefficients. If \mathbf{Z} is an invertible matrix, we can find \mathbf{I} using;

$$[I] = [Z]^{-1} \times [V] \quad (2.7)$$

2.2.1 Solving Matrix Equation

In the last part of the solution, equation (2.6) must be solved in order to find the unknown coefficients (α_i 's in Eq. (2.5)). To do so, there are three methods:

- 1) Finding the inverse of \mathbf{Z} directly or by applying inversion methods
- 2) Decomposing \mathbf{Z} into two or more simpler matrices (usually Upper and Lower Triangular matrices)
- 3) Iterative method

Once any of these methods was applied, we will find the unknown coefficients, regardless that what parameters they represent in EM. After that, depending on the

type of formulation (EFIE, MFIE or CFIE) and the parameters of the fundamental primary integral equation, (2.2) will help us to find our desired electromagnetic factors such as charge or current density distribution function.

2.2.2 Classification of MOM

In order to perform MOM algorithm, one should know how to choose basis and test functions which are the most appropriate to the nature of the problem. There are lots of mathematical functions to be used for this purpose which are defined either on a part of the object namely “Sub-domain Functions” or the “Entire-domain Functions” which are defined over the whole object.

2.2.2.1 Basis (expansion) Functions

In MOM, those groups of functions can be chosen for basis functions which are differentiable or integrable up to the degree of the operator L , but in practice, we cannot choose any function for this purpose because the mathematical operations due to applying L on them may become too complicated or sometimes impossible to solve. The noticeable point in choosing basis functions is that their behavior should be the same as the expected solution of the problem or at least they can satisfy the boundary conditions up to a certain level.

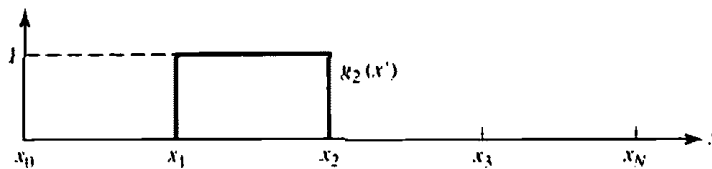
Generally in moment method, there are two types of basis functions to be used. One is the Entire Domain functions which as their name implies, are defined and nonzero over the entire length of the structure being considered. Thus no segmentation involved in their use. A common entire domain basis set is that of sinusoidal

functions, where; $f_n(x') = \cos\left[\frac{(2n-1)\pi x'}{\ell}\right]$, $-\frac{\ell}{2} \leq x' \leq \frac{\ell}{2}$.

Note that this basis set would be particularly useful for modeling the current distribution on a wire dipole, which is known to have primarily sinusoidal distribution. The main advantage of entire domain basis functions lies in problems where the unknown function may render a priori to follow a known pattern [1].

The other types of basis functions are Sub-domain functions which are defined in a specific part of the operator's domain in such a way that they are zero at the rest of the domain. The choice of basis (expansion) functions depends on the type of the problem and its complications.

Overall, the entire domain functions can be used restrictedly and they can cover a limited spectrum of the problems to analyze, while we can almost use sub-domain functions in any kind of problems, provided that we can discrete the region of operation into N similar small parts. Common sets of sub-domain functions and their illustration are as below;



Piecewise Constant

$$g_n(x') = \begin{cases} 1 & x'_{n-1} \leq x' \leq x'_n \\ 0 & \text{elsewhere} \end{cases}$$

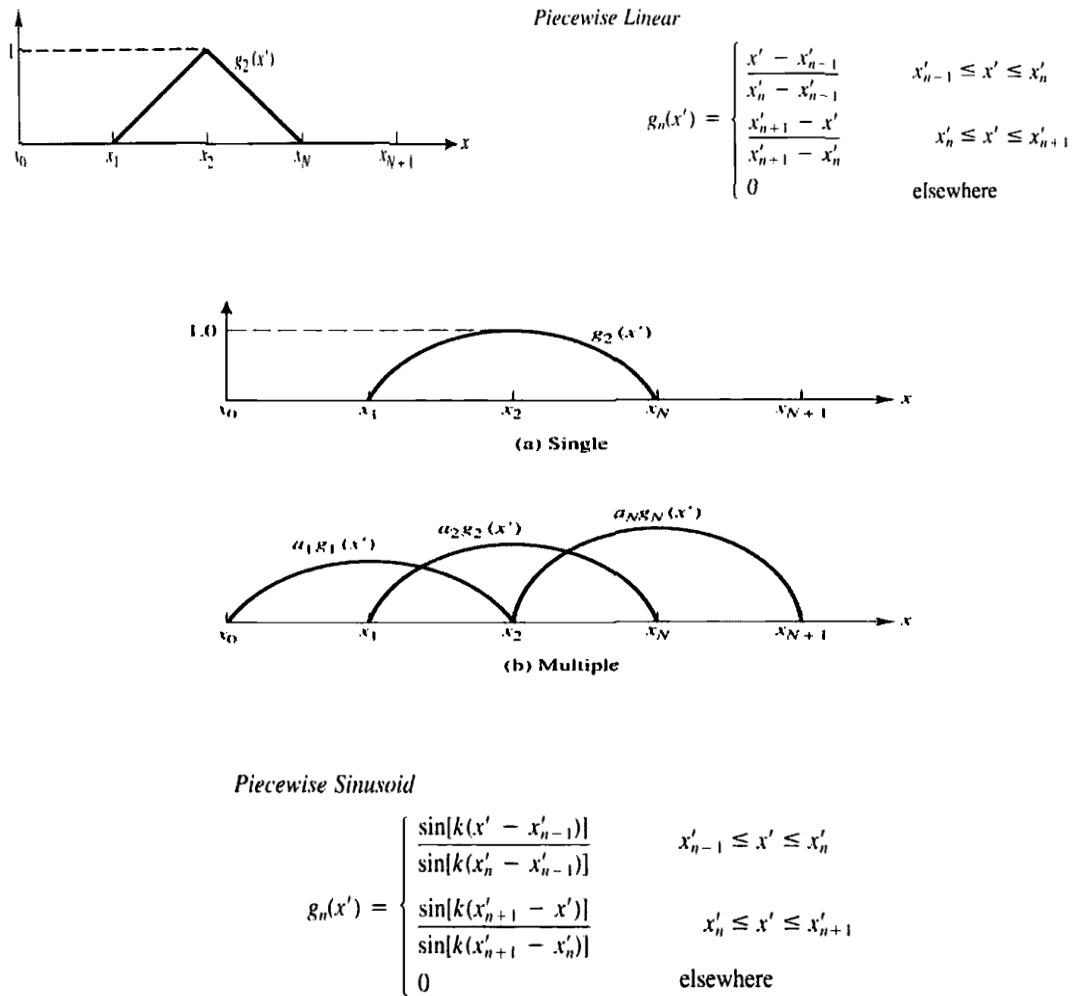


Figure 2.1: Common sub-domain basis functions [1]

2.2.2.2 Weighting (testing) Functions

In general, any function can be used as testing function, but we should be aware that if the function is too complicated, finding the elements of Z (Impedance matrix) will be hard and sometimes impossible. Two commonly used testing functions are;

- 1) Dirac-Delta function $\delta(x)$
- 2) Basis function itself

and we have;

$$\langle w \cdot g \rangle = \int w^* \cdot g$$

In the first choice, N different δ functions will be considered in N different points of the region and "dot product" (\cdot) is applied. The elements of Z and V will be found

easily because according to the property of δ function, the result of integration of the inner product of δ with any function over any region, is conditionally equal to the magnitude of the function itself at the place of δ (the condition is that the region of integration should contain the point which δ function is infinite at that point).

The process of applying the inner product of δ on Eq.(2.4) for N different points, is the same as we equate both sides of Eq.(2.4) for N different points. Hence, this method is called “Point Matching” or “Point Collocation”. It is the one of the methods which is applied in part 2.3 of this thesis.

Choosing N testing points is completely optional. They can be symmetric or asymmetric in the region of operation. The advantage of this method is simplicity in finding the elements of matrix Z .

In the second choice, basis functions are used as testing functions (i.e, $w_j = f_j$, $j=1,2,\dots,N$). This method is called “Galerkin's Method”. A great advantage of this method is its 2nd–order error.

2.2.3 Special Terms

The term "Method of Moment" is changed regarding to basis and test relations. Here are some of the most common terms:

2.2.3.1 Method of Weighting Residuals

It is derived from the following interpretation that if Eq.(3.2) in [5] represents an approximation quantity, then the difference between the exact and approximate $L(f)$'s is;

$$g - \sum_i \alpha_i L(f_i) = r$$

which is called the residual r . The inner products $\langle w_i, r \rangle$ are called the weighted residuals. Now, Eq.(1.3) in [5] is obtained by setting all weighted residuals equal to zero.

2.2.3.2 Galerkin's Method

This is when the domains of L and L^* are the same and therefore we choose $f_i = w_i$. When L is self-adjoint, this has the advantage of making our fundamental matrix symmetric. Since the treatment of a symmetric matrix is easier than a non-symmetric one, particularly for eigenvalue problems, this can be a theoretical advantage. However, Harrington claims that for computations, the evaluation of the elements of the matrix may be difficult when Galerkin's method is used, and this often outweighs the advantage of keeping the matrix symmetric [17].

2.2.3.3 Collocation Method

Perhaps the simplest mode for computation is the collocation or point matching method. This basically involves satisfying the approximate representation at discrete points in the region of interest. In terms of the method of moments, this is formally equivalent to choosing the testing (weighting) functions to be Dirac-delta functions. The integrations represented by the inner products now become trivial, which is the major advantage of this method.

2.2.3.4 Least Square Method

Another possibility is that of minimizing the length or norm of the residual, given by Eq.(3.4) in [5]. If the usual inner product is used, the procedure is called least square method. It is evident that minimization of r is equivalent to finding the shortest distance from g to the subspace generated by $L(f_i)$, $i = 1, 2, \dots, N$. Hence by the

projection theorem, the least norm is obtained by taking $w_i = L(f_i)$ in the method of moments.

There are other types of specializations such as “The Rayleigh-Rits Variational Method” and “The Perturbation Method” in which, more specifications and mathematical formulas are needed to represent their properties regarding the method of moments.

2.3 Application on Thin Wire Antenna

In this section, current distribution over a finite length dipole antenna is derived, using the moment method. The considered dipole is assumed to be very thin ($a \ll l, a \ll \lambda$) as we can call it a thin wire antenna. First step is formulating the problem in terms of an integral equation. We examine our solution for both Hallen’s and Pockkington’s integral equations. Then we solve them for the unknown current density, using both “point matching (collocation)” in section (2.3.1) and “Galerkin” form of moment method in (2.3.2).

2.3.1 Point Matching Method

The pulse function is used as our basis and Dirac-delta function as the weighting function in order to simplify HE and PE and transform them to the matrix equations which are easily solvable by MATLAB codes. The results are significantly accurate compared with the similar examples in [1].

2.3.1.1 Pocklington's Integral Equation

Consider a thin wire antenna in figure 2.2 where an incident electric field $E^i(\vec{r})$ impinges on its surface. Therefore a linear current density J_s is induced on the

surface. The induced current density will reradiate and produces a field which is referred to as the *scattered electric field* $E^s(\vec{r})$. So at any point in the space the total electric field will be $E^t(\vec{r}) = E^i(\vec{r}) + E^s(\vec{r})$.

When the antenna is transmitting, the field is generated by a voltage source connected to the terminals of the dipole at the center. There are two ways for modeling the source in our problem. First is called *delta-function generator* [DFG] which refers to an ideal generator placed in a gap between the arms of the antenna. Second one is called *magnetic frill generator* which is assumed to be a very thin disc-like generator placed at the center of the wire. For the simplicity, let's assume the first one illustrated in figure (2.2).

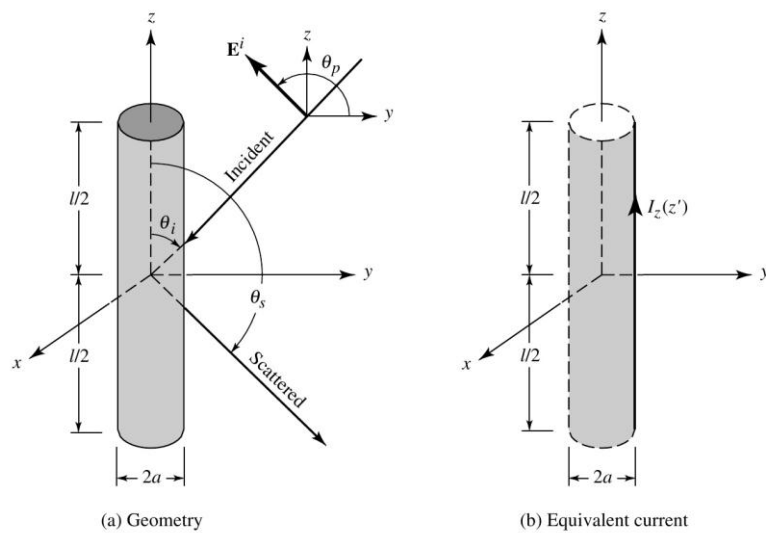


Figure 2.2: Uniform plane wave obliquely incident on a conducting wire[1]

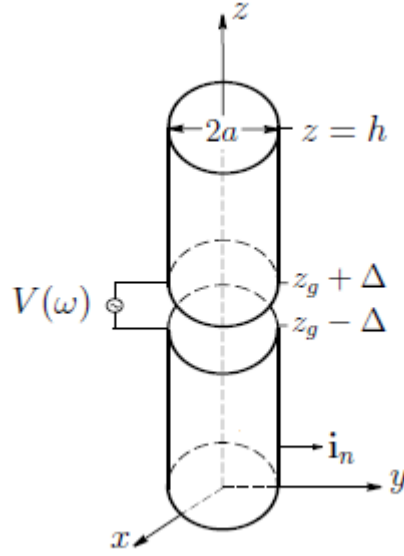


Figure 2.3: Wire Antenna with Idealized DFG[20]

When the observation point is brought onto the surface of the wire, while wire is perfectly conducting, the total tangential field vanishes;

$$E_z^t(r = r_s) = E_z^i(r = r_s) + E_z^s(r = r_s) = 0 \quad (2.8)$$

Thus, $E_z^s(r = r_s) = -E_z^i(r = r_s)$. In general, the scattered electric field generated by the current density J_s is given by:

$$\begin{aligned} E^s(r) &= -j\omega A - j \frac{1}{\omega\epsilon\mu} \nabla(\nabla \cdot A) \\ &= -j \frac{1}{\omega\epsilon\mu} [k^2 A + \nabla(\nabla \cdot A)] \end{aligned} \quad (2.9)$$

where, A is the vector (auxiliary) potential in space. However, for observation on the surface of the wire only the z -component of the field is needed which is;

$$E_z^s(r) = -j \frac{1}{\omega\epsilon\mu} [k^2 A_z + \frac{\partial^2 A_z}{\partial z^2}] \quad (2.10)$$

Since $A = \frac{\mu}{4\pi} \iint_s J_s(r) \frac{e^{-jkR}}{R} ds'$, by neglecting the edge effects we can write;

$$A_z = \frac{\mu}{4\pi} \iint_s J_z \frac{e^{-jkR}}{R} ds' = \frac{\mu}{4\pi} \int_{-l/2}^{l/2} \int_0^{2\pi} J_z \frac{e^{-jkR}}{R} a d\phi' dz' \quad (2.11)$$

If the wire is very thin, the current density J_z is not a function of the azimuthal angle

and we can write; $2\pi a J_z = I_z(z') \Rightarrow J_z = \frac{I_z(z')}{2\pi a}$

where $I_z(z')$ is assumed to be an equivalent filament line-source current located a radial distance $\rho = a$ from the z -axis, as shown in figure 2.4. Therefore, Eq.(2.11) reduces to;

$$A_z(\rho = a) = \mu \int_{-l/2}^{l/2} I_z(z') G(z, z') dz' \quad (2.12)$$

where $G(z, z') = \int_0^{2\pi} \frac{e^{-jkR}}{R} d\phi'$ and

where; $R = \sqrt{(x-x')^2 + (y-y')^2 + (z-z')^2} = \sqrt{(\rho^2 + a^2 - 2\rho a \cos(\phi - \phi')) + (z-z')^2}$

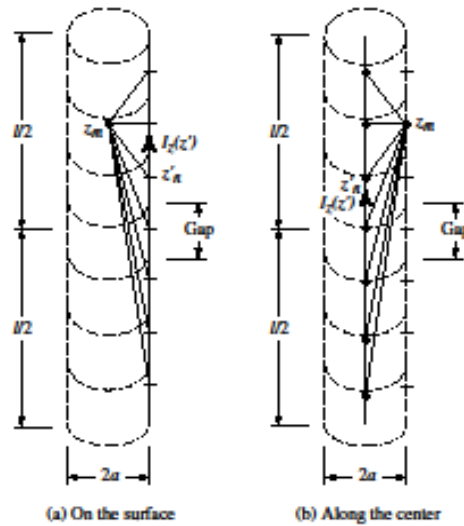


Figure 2.4: Dipole segmentation and its equivalent current [1]

while ρ is the radial distance to the observation point and a is the radius. Figure 2.5 shows the segmentation on the wire antenna.

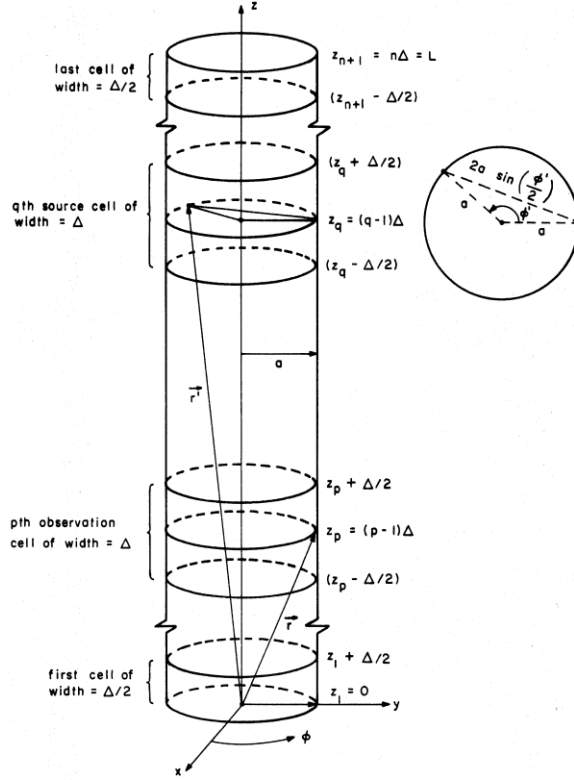


Figure 2.5: Geometry of the problem showing the zoning of the antenna[15]

Because of the symmetry of the wire, the observations are not a function of ϕ . For simplicity let us choose $\phi = 0$. Hence;

$$R(\rho = a) = \sqrt{4a^2 \sin^2\left(\frac{\phi'}{2}\right) + (z - z')^2}$$

Now from Eq.(2.8) and (2.10) we have

$$-j \frac{1}{\omega \epsilon} \left(k^2 + \frac{d^2}{dz^2}\right) \int_{-l/2}^{l/2} I_z(z') G(z, z') dz' = -E_z^i(\rho = a) \quad (2.13)$$

or

$$\left(k^2 + \frac{d^2}{dz^2}\right) \int_{-l/2}^{l/2} I_z(z') G(z, z') dz' = -j\omega \epsilon E_z^i(\rho = a) \quad (2.14)$$

Interchanging integration with differential equation we can write;

$$\int_{-l/2}^{l/2} I_z(z') \left[\left(k^2 + \frac{d^2}{dz'^2} \right) G(z, z') \right] dz' = -j\omega\epsilon E_z^i(\rho = a) \quad (2.15)$$

Equation (2.15) is referred to as *Pocklington's integral equation* which can be used to determine the equivalent filamentary line-source current and thus current density on the wire, by knowing the incident field on the surface of the wire [1]. If we assume

that the wire is very thin such that $a \ll \lambda$ so we can write $G(z, z') = \frac{e^{-jkR}}{4\pi R}$, Eq.(2.15)

can be expressed as;

$$\int_{-l/2}^{l/2} I_z(z') \frac{e^{-jkR}}{4\pi R^5} [(1 + jkR)(2R^2 - 3a^2) + k^2 a^2 R^2] dz' = -j\omega\epsilon E_z^i(\rho = a) \quad (2.16)$$

2.3.1.2 Hallen's Integral Equation

Referring to figure (2.4), as $a \ll \lambda$ and $a \ll l$ so that the effects of the end faces of the wire can be neglected, according to the boundary conditions and the assumption of perfect conductivity of the arms, we can say that total tangential E field at the surface of the wire and the currents at the end surfaces of the cylinder are vanished.

Since the current induced on the surface of the wire in the direction of a_z , we can write;

$$E_z^t = -j\omega A_z - j \frac{1}{\omega\epsilon\mu} \frac{\partial^2 A_z}{\partial z^2} = -j \frac{1}{\omega\epsilon\mu} \left[\frac{d^2 A_z}{dz^2} + \omega^2 \epsilon\mu A_z \right]$$

since the total tangential electric field is zero on the surface of the cylinder, above

equation is reduced to;

$$\frac{d^2 A_z}{dz^2} + k A_z = 0 \quad (2.17)$$

Because the current density is symmetrical on the wire, A_z is also symmetrical. So the solution for the above differential equation is;

$$A_z(z) = -j\sqrt{\varepsilon\mu}[B\cos(k|z|) + C\sin(k|z|)] \quad (2.18)$$

where B and C are constants. Also for a current-carrying wire, its potential is given

by $A_z(z') = \int_{-l/2}^{l/2} I_z(z') \frac{e^{-jkR}}{4\pi R} dz'$, hence;

$$\int_{-l/2}^{l/2} I_z(z') \frac{e^{-jkR}}{4\pi R} dz' = -\frac{j}{\eta}[B\cos(k|z|) + C\sin(k|z|)] \quad (2.19)$$

where $\eta = \sqrt{\mu/\varepsilon}$ is the intrinsic impedance of the conductor. If the applied voltage at the terminals of the antenna is V_i it can be shown that $C = V_i/2$ while B can be found by applying the boundary condition at the end surfaces of the cylindrical wire. Equation (2.19) is referred to as *Hallen's integral equation* for a perfectly conducting wire.

2.3.1.3 Moment Method Solution

After formulating the problem in terms of Hallen and Pocklington's integral equations we can modify the integral form into the matrix equation. To do so, let us divide the wire uniformly to N equal segments each by height $\Delta = l/N$ as shown in figure (2.5). Now for applying the point matching form of MOM we take observation (field) points (or matching points) z_m at the midpoint of each subinterval as it is

shown in the figure below where the positions of z_m 's and z_n 's are; $z_n = \frac{(n-1)l}{N}$

and $z_m = \frac{(2m-1)l}{2N}$, $m = 1, 2, \dots, N+1$

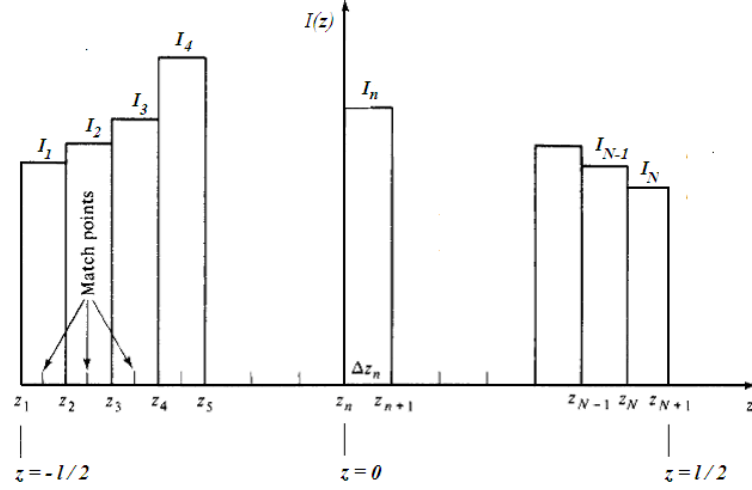


Figure 2.6: Wire antenna with N segments

Then we approximate $I(z)$ as $I(z) \approx \sum_{n=1}^N I_n P_n(z)$. Refer to moment method solution,

P_n 's are our basis functions. Let us take them as pulse functions;

$$P_n(z) = \begin{cases} 1 & , z_n \in \Delta z \\ 0 & , z_n \notin \Delta z \end{cases}$$

Substituting $I(z)$ in Hallen's integral equation yields;

$$\sum_{n=1}^N I_n \int_{-l/2}^{l/2} G(z_m, z') P_n(z') dz' = -\frac{j}{\mu} B \cos(kz_m) - \frac{j}{2\mu} \sin(k|z_m|) \quad (2.20)$$

or

$$\sum_{n=1}^N I_n \int_{z_n}^{z_{n+1}} G(z_m, z') dz' = -\frac{j}{\mu} B \cos(kz_m) - \frac{j}{2\mu} \sin(k|z_m|) \quad , m = 1, 2, \dots, N+1 \quad (2.21)$$

which is $[A_{mn}][I_n] = [e_m]$ in its matrix form where;

$$A_{mn} = \int_{-l/2}^{l/2} G(z_m, z') dz' \quad \text{and} \quad e_m = -\frac{j}{\mu} B \cos(kz_m) - \frac{j}{2\mu} \sin(k|z_m|)$$

The point is that the value for B is unknown. Applying boundary condition on current at $z=l$ is imposed as $I_n = 0$. Then C must be treated as an unknown in the system of linear equation previously formed by our matrix equation. Therefore the matrix equation is in the form;

$$\begin{pmatrix} A_{11} & A_{12} & \cdots & A_{1,N-1} & d_{1N} \\ A_{21} & A_{22} & \cdots & A_{2,N-1} & d_{2N} \\ \vdots & \vdots & \ddots & \vdots & \vdots \\ A_{N1} & A_{N2} & \cdots & A_{N,N-1} & d_{N,N} \end{pmatrix}_{N \times N} \begin{pmatrix} I_1 \\ I_2 \\ \vdots \\ I_{N-1} \\ B \end{pmatrix}_{N \times 1} = \begin{pmatrix} b_1 \\ b_2 \\ \vdots \\ b_{N-1} \\ b_N \end{pmatrix}_{N \times 1} \quad (2.22)$$

where; $d_m = -\frac{j}{\eta} \cos(kz_m)$, $b_m = -\frac{j}{2\eta} \sin(k|z_m|)$

Hence by solving the above equation, current distributions induced over the surface of the thin wire (dipole) antenna which is extracted using Hallen's integral equation, pulse basis function and the point matching procedure, agrees quite well with the experimental results [33]. Let us solve an example to see the result.

Problem 1- Using Hallen's IE, determine the current distribution $I(z)$ on a straight dipole of length ℓ . Plot $|I| = |I_{re} + j I_{img}|$ against z . Assume excitation by a unit voltage, $N = 51$, $\Omega = 2 \ln(\ell/a) = 12.5$, and consider cases: (a) $\ell = \lambda/2$, (b) $\ell = 1.5 \lambda$ (problem 5.23 from [28]).

Solution, using the above procedure would result into the figure below;

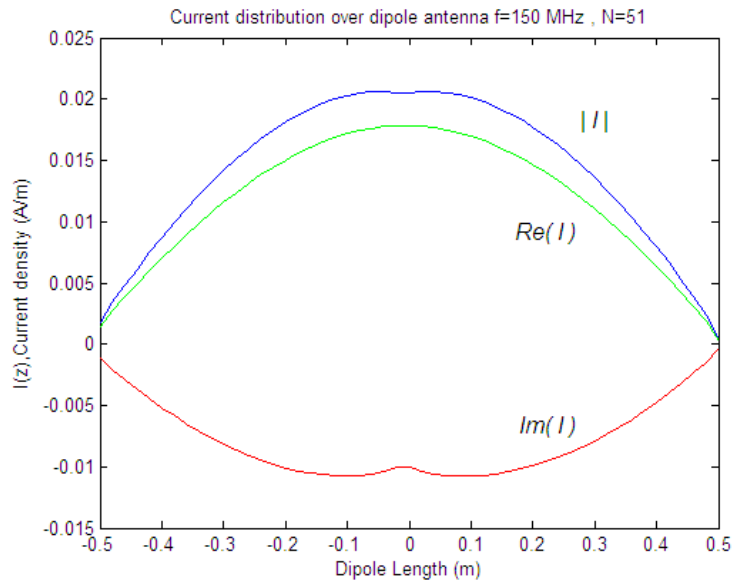


Figure 2.7: Current distribution, part (a) where; $\lambda = 2(m), \ell = \lambda/2$

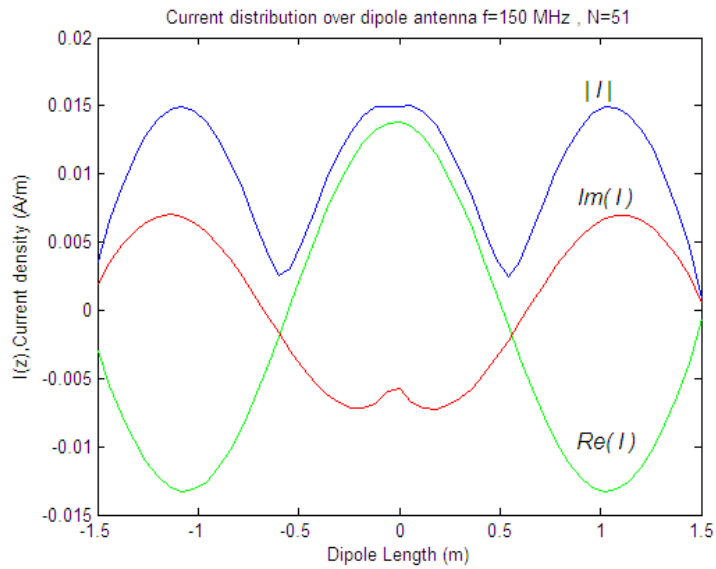


Figure 2.8: Current distribution, part (b) where; $\lambda = 2(m), \ell = 1.5\lambda$

In this example, basis functions are assumed to be sub-domain pulse functions and Dirac-delta functions as testing functions are used, hence the term point matching (collocation) implied. Figures (2.7) and (2.8) illustrate desired current distribution over the surface of the thin wire dipole with characteristics in problem1.

Observations are analogous to the results demonstrated in [28]. We can observe that in figure (2.7) the current is distributed sinusoidally (as it was expected) with a good approximation over all parts of the wire except at the end points where it should be zero according to the boundary conditions explained previously.

Our second problem (example 8.4 from [1]) is to compare the results when piecewise constant (pulse) sub-domain basis functions and point matching are used for both Hallen's IE and Pocklington's IE.

Problem 2- Assume a center-fed linear dipole of $l = 0.47\lambda$ and $a = 0.005\lambda$. Determine the normalized current distribution over the length of the dipole using $N=21$ segments to subdivide the length. Plot the current distribution. Use Pocklington's integrodifferential equation to solve the problem.

Because the current at the ends of the wire vanishes, the piecewise constant sub-domain basis functions are not the most judicious choice. However, because of the simplicity, they are chosen here to illustrate the principles even though the results are not the most accurate.

Assume the excitation voltage $V_i = 1v$ [1].

Using the same process, the results are as follows;

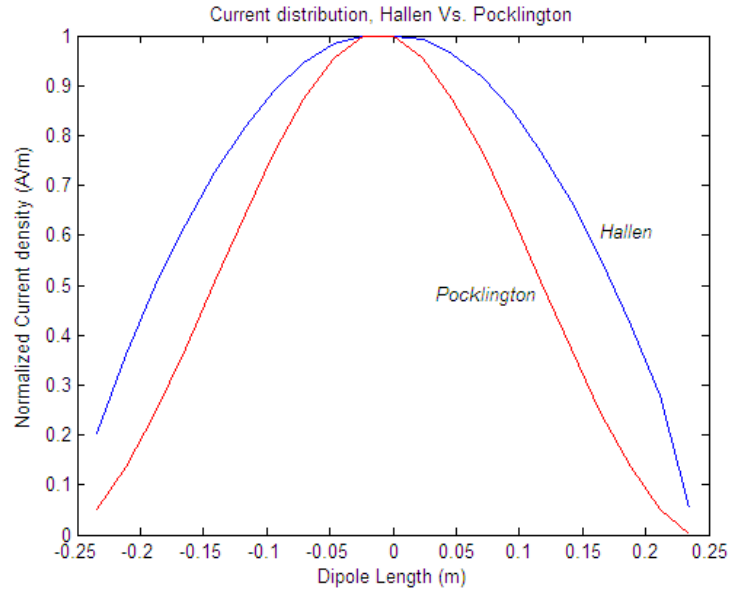


Figure 2.9: Current distribution, $\lambda = 1(m), \ell = 0.47\lambda$.

The figure above shows that the solution by using both integral equations and point matching with pulse basis functions (and Dirac-delta test functions) are satisfactory. However, as current must vanish at the end points (whereas we have currents as above) it shows that piecewise constant basis functions are not judicious ones to be taken as the basis functions. Overall, the results near the feeding point are perfectly matched with the assumption of sinusoidal current distribution over a wire with $l = \lambda / 2$.

Moreover, the result extracted from Pocklington's IE gives better convergence at the feeding point, though it takes more time to be computed because of the complexity in Eq.(2.15) or (2.16). Also it provides more accurate result at the end points of the wire than the one in which using Hallen's IE was used.

2.3.2 Galerkin Method

As it was mentioned in section 2.2.3.2, it is referred to this method when an identical function is used for both basis and testing functions. Here in this part, we use an Entire-domain cosine function and compare the results for both HE and PE equations with the ones we've found for point-matching method and the ones which are in some references.

The process of transformation of the equations to the matrix equation forms are the same as the previous ones. But the formulation of the problems is a bit different due to the limitations that arise from using entire-domain function.

2.3.2.1 Hallen's Integral Equation

To get started, consider Hallen's equation of the form;

$$\int_{-h}^h G(z, z') I(z') dz' = -\frac{j}{2\eta} \sin(k|z|) + C \cos(kz) \quad (2.23)$$

where h denotes the one arm length of the antenna. Fikioris [13] suggests a numerical method consisting $I(z) = I^{(1)}(z) + CI^{(2)}(z)$ where $I^{(1)}(z)$ satisfies eq.(2.23) with the right hand side containing only the sine component and $I^{(2)}(z)$ satisfying the equation with the right hand side containing only the cosine component. The solution for Galerkin method with entire domain basis function $\cos(n\pi z/h)$ with $n=0, 1, \dots, N$ leads to two $(N+1) \times (N+1)$ systems of equations for the basis function coefficients $I_n^{(1)}$ and $I_n^{(2)}$.

Once the two systems were solved, we determine C as;

$$C = - \frac{\sum_{n=0}^N (-1)^n I_n^{(1)}}{\sum_{n=0}^N (-1)^n I_n^{(2)}}$$

and the final current approximation on the wire which vanishes at end points of the antenna takes the form;

$$I(z) \cong \sum_{n=0}^N [I_n^{(1)} + CI_n^{(2)}] \cos\left(\frac{n\pi z}{h}\right) \quad (2.24)$$

Galerkin solution to problem 1 in section 2.3.1.3 with N=40 segments yields the following figure;

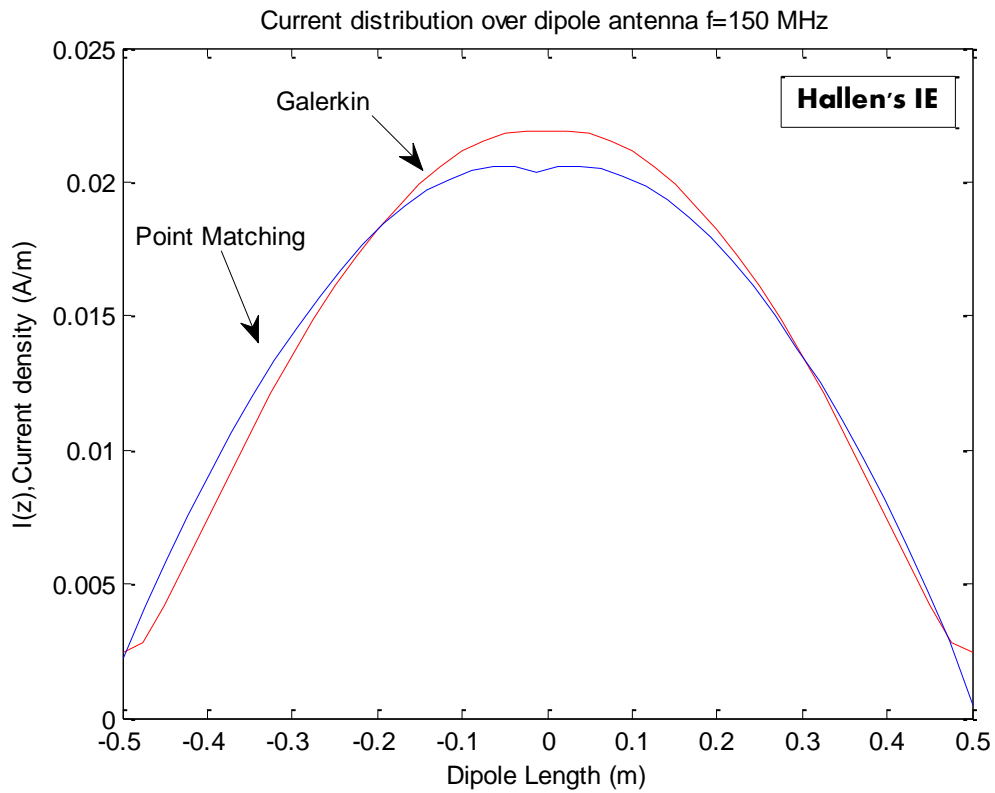


Figure 2.10: Current distribution, Galerkin vs. Point matching (HE)

Figure (2.10) shows that the distribution over the wire antenna is almost the same for Galerkin and Point matching, but point matching applies the boundary condition better than Galerkin at the end points (hence the name Point Matching).

Hallen's solution for a thin wire antenna ($h = 0.25\lambda, a = 0.01\lambda$) with $N=40$ evaluation points of current are illustrated in figures (2.11) and (2.12).

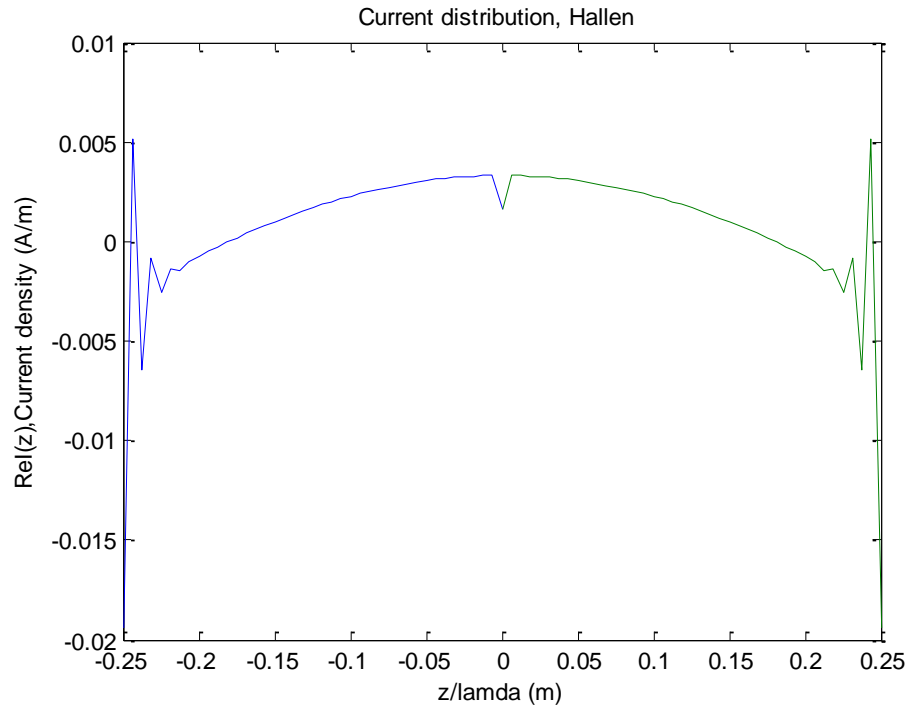


Figure 2.11: Current distribution (real) over the dipole

The figure above shows the real part of the current distribution on the dipole antenna. The most abnormal behavior of using Galerkin method with entire-domain functions in this particular example is the rapid oscillations that occur at the end points for real part and the imaginary part of the current especially at the center of dipole where it is fed.

Fikioris [13] claims that these oscillations will decrease when the Delta-Function Generator (DFG) is replaced by the equivalent Frill-Generator(FG). Also, there is a discussion about the relation between the radius of the wire antenna and the number of segments to be chosen (see [13]).

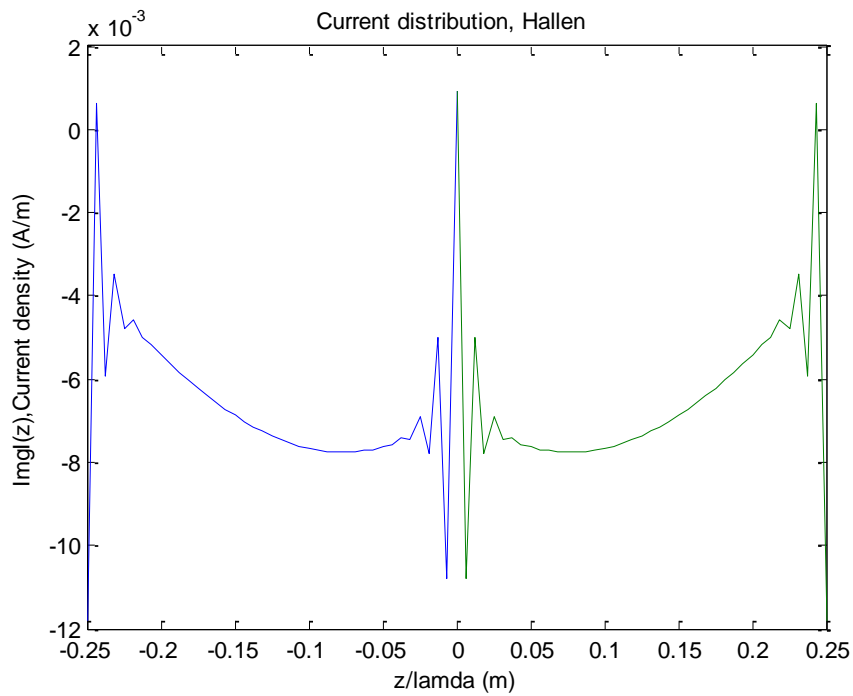


Figure 2.12: Current distribution (imaginary) over the dipole

For the coefficients of the basis functions we also illustrate the results in figures (2.13) and (2.14), to observe their variances along the wire. The real parts of the coefficients appear to oscillate about $z=0$ while the behavior of the imaginary parts seems to grow eventually in magnitude.

The behavior of real part coefficients is associated with the oscillations near end points of the current whereas the behavior of imaginary part is associated with the oscillations near the center point in imaginary current.

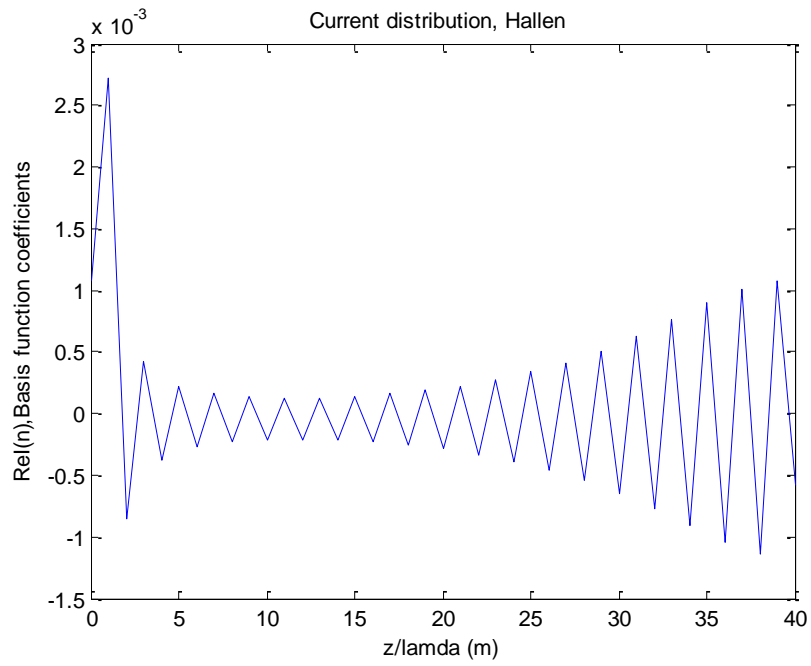


Figure 2.13: Coefficients of the basis functions (real)

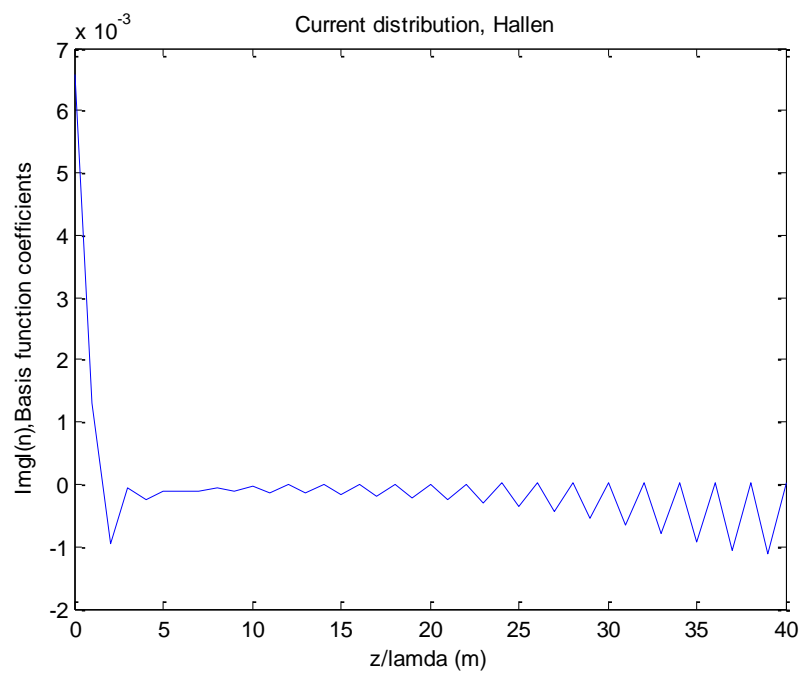


Figure 2.14: Coefficients of the basis functions (imaginary)

2.3.2.2 Pocklington's Integral Equation

Considering PE and Galerkin method, both formulation and numerical technique are the same as the point-matching. The only difference is the basis and test functions which are identical and has the form of entire-domain basis function $\cos(n\pi z/h)$.

Obviously, dissimilar to the Hallen's case, the integrand would take more components and this yields to more complicated and time consuming evaluation of the impedance matrix elements and its inverse to solve the equation for current distribution.

2.3.2.3 Moment Method Solution

From equations (2.16), (2.17), (2.18) and the fact that the potential of a current

carrying wire is given by $A_z(z') = \int_{-l/2}^{l/2} I_z(z') \frac{e^{-jkR}}{4\pi R} dz'$ we can write;

$$\int_{-l/2}^{l/2} I_z(z') \frac{e^{-jkR}}{4\pi R^5} [(1 + jkR)(2R^2 - 3a^2) + k^2 a^2 R^2] dz' = -\frac{j}{2\eta} \sin(k|z|) + C \cos(kz)$$

Next step is to substitute $I(z') = \sum_{n=0}^N I_n \cos\left(\frac{n\pi z'}{h}\right)$ and inner product both sides of the

above equation with the same weighting function $\cos\left(\frac{n\pi z}{h}\right)$ in order to form the

matrix equation.

Then using the same technique of Fikioris [21], current distribution on the thin wire antenna using Pocklington's integral equation and Galerkin with entire-domain basis function would be as the one illustrated in figure (2.14) and (2.15) for real and imaginary parts of the current.

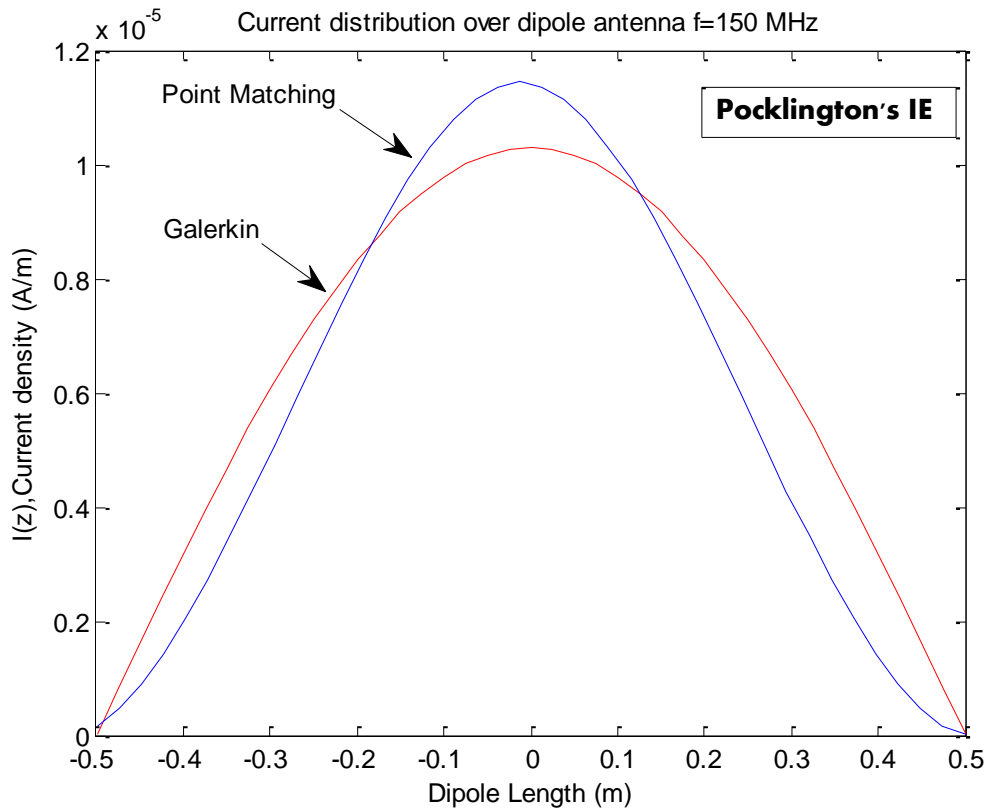


Figure 2.15: Current distribution, Galerkin vs. Point matching (PE)

From the figure above, we can see that solution of PE using an entire domain sinusoidal basis and test functions (Galerkin) is representing sinusoidal distribution over the antenna more than using pulse and dirac-delta functions (point matching). Moreover, solution of PE holds the boundary conditions at the antenna end points more than HE, especially in case of applying Galerkin method.

After solving various examples of MOM application on the thin wire antenna for unknown current distribution, we have noticed that even by using fast computers, numerical solution for such n-body problems has the order of $O(N^2)$ complexity with the large amount of memory consumption to store the data in order to use them for the other desirable parameters.

For example, to solve a matrix equation in our problems, we first generate the impedance matrix, then calculate its inverse and multiply this inverse matrix by both sides of the equation which is extremely expensive considering time and memory, especially when the number of unknowns is quite large which is case for big structures in the real life.

Therefore, in the next chapter, we are going to introduce one of the most popular fast algorithm called “Fast Multipole Method (FMM)” to achieve the recent solutions, using less time and memory allocations. In chapter 4, the combination of FMM with Point-matching and Galerkin methods are applied for the particular problems of solving Hallen’s and Pocklington’s integral equations.

Chapter 3

Fast Multipole Method (FMM)

3.1 Introduction to FMM

Fast Multipole Method (FMM) introduced first time by Greengard and Rokhlin for 2D and 3D problems, to reduce the computational complexity of N -body problems by applying an error-controlled approximation technique to the Green's function of a system. It allows the interaction due to a group of particles to be computed as if there is a single particle.

When FMM is applied to vector electromagnetic problems, the interaction between well-separated groups of basis functions can be evaluated very quickly. This will lead to a rapid calculation of matrix-vector product in an iterative solver without storing many of the matrix elements. Hence, this technique speeds up the calculation and reduces the amount of memory needed for solving all type of such problems [14].

Here in this thesis, the Green's function under consideration is the Green's function for Helmholtz equation and obviously we are going to examine FMM application on a one dimensional problem of thin wire antenna.

Later on in chapter 4, when we modify this method for our MOM solution of the wire antenna, we will see that FMM is not only useful to speed up the multiplication

of $Z^{-1}V$, but it is also useful to accelerate evaluation of the impedance matrix Z and facilitate the computation of inverse impedance matrix in this particular problem which is finding the current distribution on the DFG fed thin dipole antenna.

For now, let us focus on the basic concepts of general FMM algorithm and the steps of forming a FMM solution.

3.2 Basic Concepts

Many problems in physics (computation of electrostatic or gravitational potentials and fields), molecular dynamic simulations, fluid mechanics and density estimation are based on the pairwise interaction models between particles in one or two domains of the form;

$$f(y) = \sum_{i=1}^N q_i K(y - x_i)$$

where K is a known kernel or green function, q_i 's are scalar values and $\{x_i\}$ is a set of “source points” and y is a “target point”. To evaluate f for a set of target points $\{y_j\}$, there is a need for $N \times N$ calculation. Typically, the applications of interest involve the evaluation of f at the same locations x_i with the self-interaction term omitted);

$$f(x_j) = \sum_{i \neq j}^N K(x_j - x_i)$$

To do so, FMM suggests to divide the domain of f into particular number of sets containing numbers of source points as well as target points which are close to each other in some dimensions so we can treat them as a single source point and name the interaction between adjacent groups as “near field” interaction (near, while the

interaction between the groups which are not close to each other is called “far field” interaction.

The process of making sets is called “spatial grouping”. Separation of the sets is very crucial because the separation parameter controls the efficiency of our fast summation by means of the accuracy since the truncation number depends on this parameter substantially.

The near field interaction and target point evaluation is to be performed by the regular pairwise interactions. For the approximation of far field evaluation, we perform three steps of *aggregation*, *translation* and *disaggregation*.

These steps are based on the degeneration of the kernel K . The process of aggregation is to relate the source points in one group with a point in group which is usually located at the center of the group by means of some functions.

After this process is done for all groups, we form a groupwise set of interactions between any two (non-adjacent) group centers to evaluate the effects of points in one group on the other one referred to translation operation. Note that this process is performed only between the group centers regardless of point source locations. The final step is to expand the value found at the center of target group to each individual member (target points) of that group.

Generally, in FMM there are two types of spatial grouping. One is to group both source and target points as described above. The other one is to group only target points or source points. In the recent one, regarding to the final step of FMM, there

are two different expansions; “local (near field) expansion” and “multipole (far field) expansion”. To have a better understanding, let us show this process by some figures.

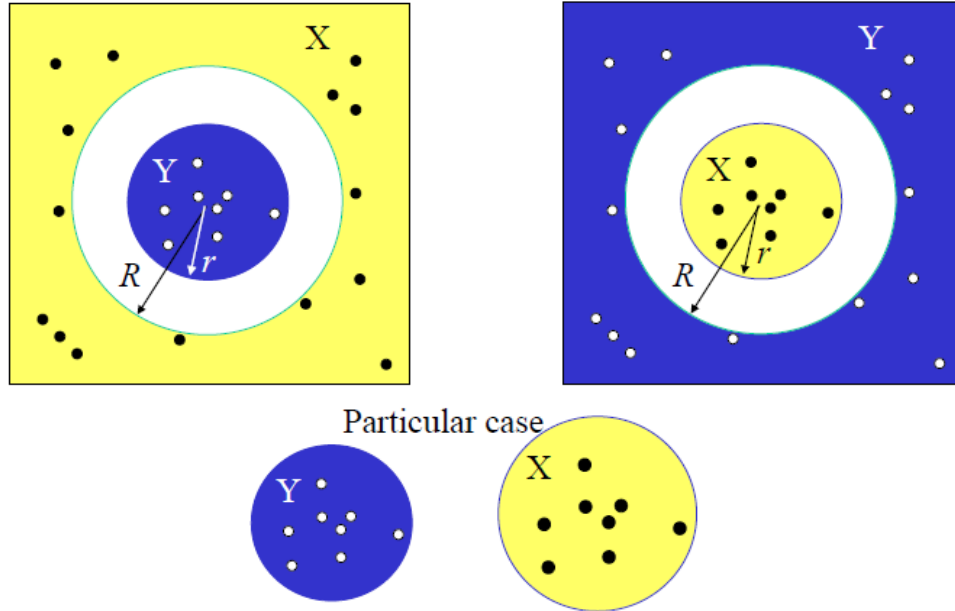


Figure 3.1: Well-separated sets

In figure above, X and Y denote the source and target points respectively.

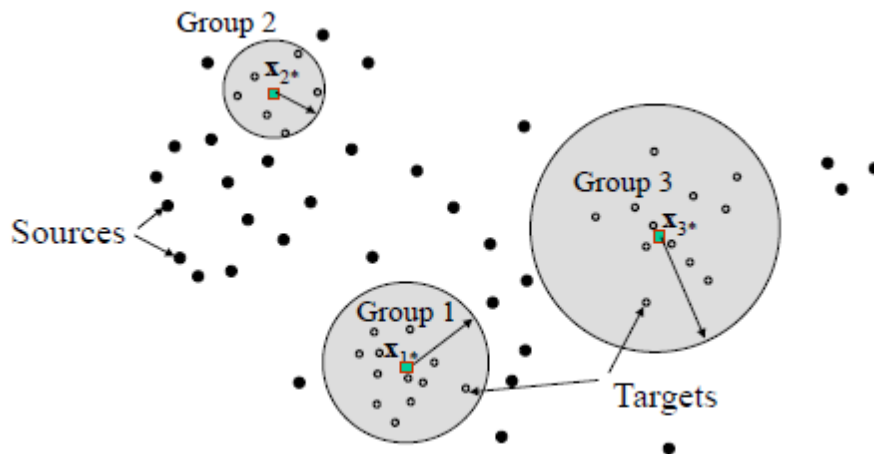


Figure 3.2: Grouping with respect to the target sets

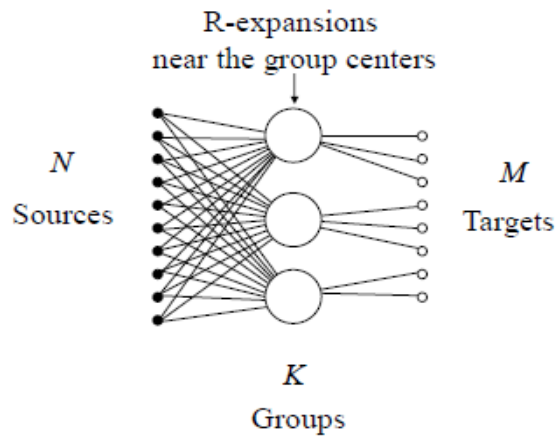


Figure 3.3: Local expansion

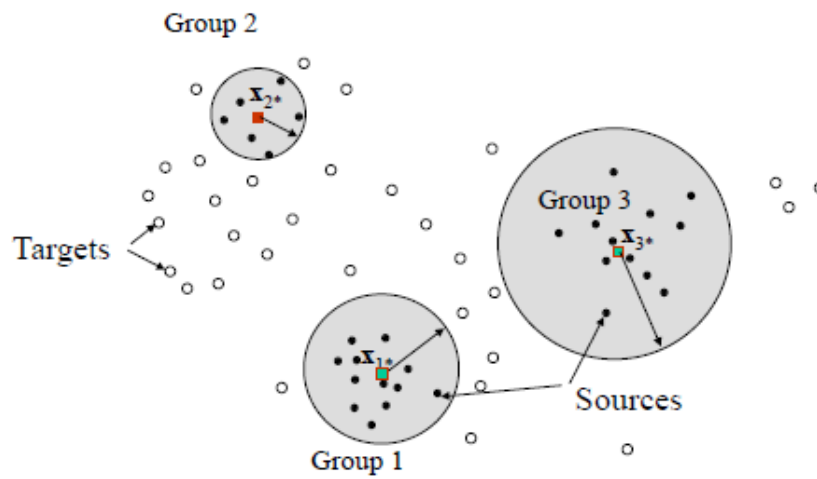


Figure 3.4: Grouping with respect to the source sets

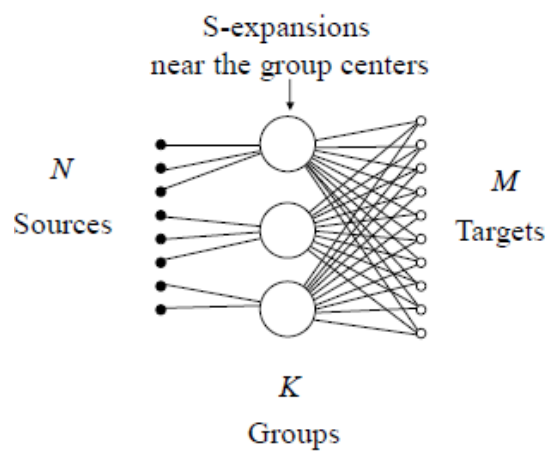


Figure 3.5: Far field expansion

As it was mentioned previously, for expansion we group both source and target points and we use a translation function to translate the interactions between the elements and the center in one group to another group center.

It is to say that FMM is performed in two forms. One is called “Single Level Fast Multipole Method” (SLFMM) in which we break the domain into particular number of sets for sources and targets only one time. The second form is called “Multilevel Fast Multipole Method” (MLFMM) which goes some steps further than SLFMM and groups the derived sets from SLFMM onto some certain levels using hierarchical tree-codes.

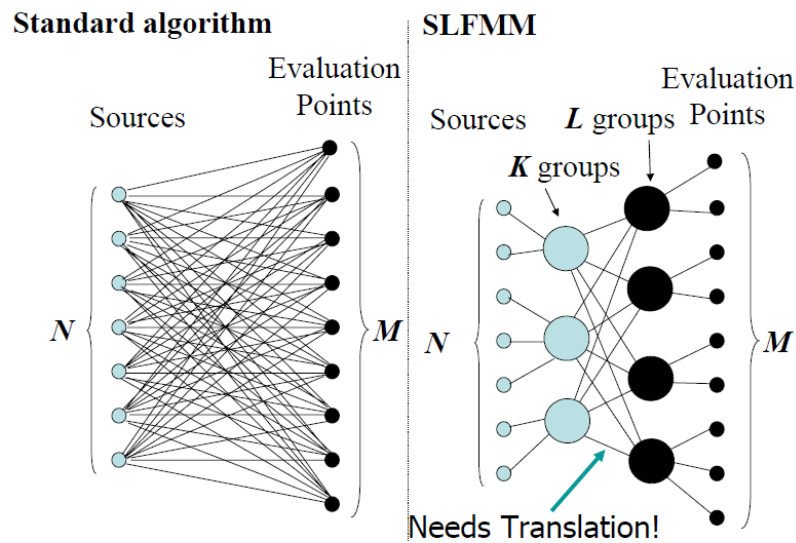


Figure 3.6: Standard and single level FMM

While total number of operations for standard algorithm is in the order of $O(NM)$, the total number of operations for SLFMM is in the order of $O(N+M+KL)$.

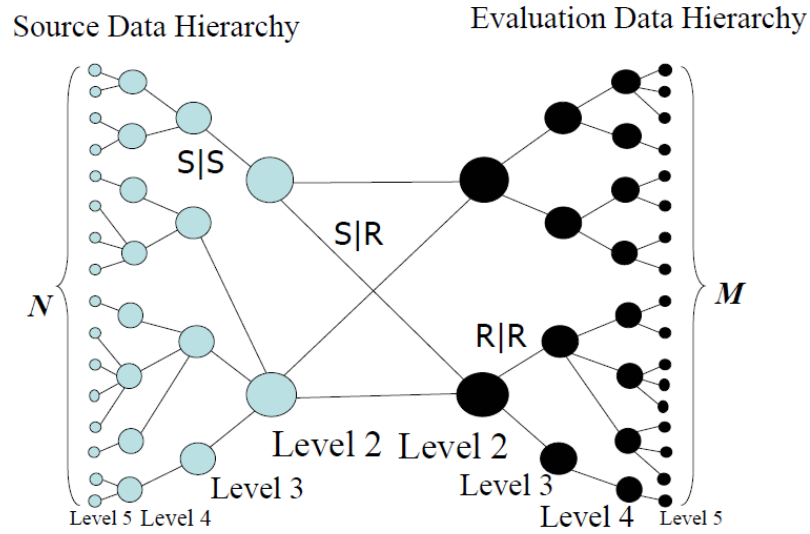


Figure 3.7: MLFMM using hierarchical clustering of domain

In the figure above S and R denote far field and local expansions. $S|S$, $R|R$ and $S|R$ terms are multipole-to-multipole, local-to-local and multipole-to local translations respectively.

Looking to the recent two figures, it is more understandable that why FMM has become a popular algorithm for solving large N -body problems. It can break the number of operations needed for the solution significantly into a few operations, saving time and memory.

3.3 Degenerating Kernel

After an overview of FMM algorithm, it is time to see how we can derive aggregation, translation and disaggregation operators for two separated sets which are far away from each other in a particular equation's kernel (which in our case, it is Green's function of Helmholtz equation, without the $1/(4\pi)$ constant).

Assume the kernel of the form;

$$G(\mathbf{r}, \mathbf{r}') = \frac{e^{-jk(|\mathbf{r}-\mathbf{r}'|)}}{|\mathbf{r}-\mathbf{r}'|} \quad (3.1)$$

where \mathbf{r}' and \mathbf{r} are the source and observation points respectively. This kernel is called separable or degenerate if;

$$G(\mathbf{r}, \mathbf{r}') = \sum_{l=1}^L f_l(\mathbf{r}) g_l(\mathbf{r}') \quad (3.2)$$

We need this degeneration, to represent eq.(3.1) in form of matrix multiplication which is required to solve our problem. Let us modify eq.(3.1) by adding a small offset \mathbf{d} to the source location. Then;

$$\frac{e^{-jk|\mathbf{r}-\mathbf{r}'+\mathbf{d}|}}{|\mathbf{r}-\mathbf{r}'+\mathbf{d}|} = \frac{e^{-jk|\mathbf{D}+\mathbf{d}|}}{|\mathbf{D}+\mathbf{d}|} \quad (3.3)$$

where $\mathbf{D}=\mathbf{r}-\mathbf{r}'$. From the definition of *Spherical Hankel function of the Second kind* and using *addition theorem* for the spherical waves [4];

$$\frac{e^{-jk|\mathbf{D}+\mathbf{d}|}}{|\mathbf{D}+\mathbf{d}|} = -jk \sum_{l=0}^L (-1)^l (2l+1) J_1(k|\mathbf{d}|) h_l^{(2)}(k|\mathbf{D}|) P_l(\hat{\mathbf{d}} \cdot \hat{\mathbf{D}}) \quad (3.4)$$

where $J_1(x)$ is the spherical Bessel function of the first kind and $P_l(x)$ is the legendre polynomial of order l . According to [14] we can convert eq.(3.4) to a surface integral on the unit sphere through the relationship;

$$4\pi(-j^l) J_1(k|\mathbf{d}|) P_l(\hat{\mathbf{d}} \cdot \hat{\mathbf{D}}) = \iint_1 e^{-jk\hat{\mathbf{k}} \cdot \mathbf{d}} P_l(\hat{\mathbf{k}} \cdot \hat{\mathbf{D}}) dS \quad (3.5)$$

where $\hat{\mathbf{k}}$ is unit radial vector on the surface of sphere. Using eq.(3.5) we can write;

$$\frac{e^{-jk|\mathbf{D}+\mathbf{d}|}}{|\mathbf{D}+\mathbf{d}|} = \frac{k}{4\pi} \iint_1 e^{-jk\hat{\mathbf{k}}\cdot\mathbf{d}} \sum_{l=0}^{\infty} (-j)^{l+1} (2l+1) h_l^{(2)}(k|\mathbf{D}|) P_l(\hat{\mathbf{k}}\cdot\hat{\mathbf{D}}) dS \quad (3.6)$$

where the summation will be truncated at some finite order L (truncation number) which limits the acceptable value for \mathbf{D} and \mathbf{d} . Hence;

$$\frac{e^{-jk|\mathbf{D}+\mathbf{d}|}}{|\mathbf{D}+\mathbf{d}|} = \frac{k}{4\pi} \iint_1 e^{-jk\hat{\mathbf{k}}\cdot\mathbf{d}} T_L(k, \hat{\mathbf{k}}, \mathbf{D}) dS \quad (3.7)$$

with,

$$T_L(k, \hat{\mathbf{k}}, \mathbf{D}) = \frac{k}{4\pi} \sum_{l=0}^L (-j)^{l+1} (2l+1) h_l^{(2)}(k|\mathbf{D}|) P_l(\hat{\mathbf{k}}\cdot\hat{\mathbf{D}}) \quad (3.8)$$

which is referred to as *transfer function* or translation operator. This transfer function converts the outgoing waves radiating from a source point to a set of incoming spherical waves at an observation point[14].

Now consider figure(3.8), where points α and β are two observation and source points respectively, close to (in terms of wave length) \mathbf{r} and \mathbf{r}' and the vector $\mathbf{v}=\mathbf{r}-\mathbf{r}'$.

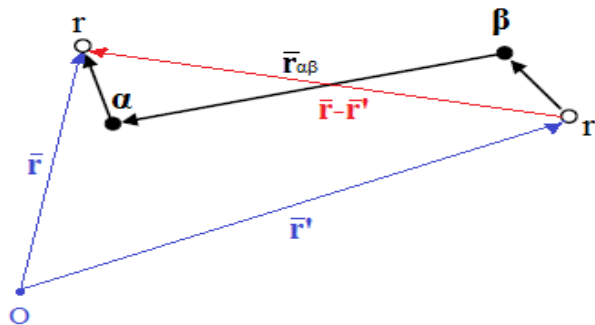


Figure 3.8: Vector translation

we can write;

$$\mathbf{v} = (\mathbf{r} - \alpha) + (\alpha - \beta) + (\beta - \mathbf{r}')$$

or

$$\mathbf{v} = \mathbf{r}_{r\alpha} + \mathbf{r}_{\alpha\beta} - \mathbf{r}_{r'\beta}$$

Using the above and eq.(3.7) rewriting the Green's function and taking a summation over it for N source points yields;

$$\sum_{n=1}^N \frac{e^{-jk|\mathbf{r}-\mathbf{r}_n|}}{|\mathbf{r}-\mathbf{r}_n|} = \iint_1 \sum_{n=1}^N e^{-jk\hat{\mathbf{k}}\cdot(\mathbf{r}_{r\alpha}-\mathbf{r}_{r_n\beta})} T_L(k, \hat{\mathbf{k}}, \mathbf{r}_{\alpha\beta}) dS \quad (3.9)$$

which is;

$$\sum_{n=1}^N \frac{e^{-jk|\mathbf{r}-\mathbf{r}_n|}}{|\mathbf{r}-\mathbf{r}_n|} = \iint_1 \sum_{n=1}^N e^{-jk\hat{\mathbf{k}}\cdot\mathbf{r}_{r\alpha}} T_L(k, \hat{\mathbf{k}}, \mathbf{r}_{\alpha\beta}) e^{jk\hat{\mathbf{k}}\cdot\mathbf{r}_{r_n\beta}} dS \quad (3.10)$$

with transfer function;

$$T_L(k, \hat{\mathbf{k}}, \mathbf{r}_{\alpha\beta}) = \frac{k}{4\pi} \sum_{l=0}^L (-j)^{l+1} (2l+1) h_l^{(2)}(k|\mathbf{r}_{\alpha\beta}|) P_l(\hat{\mathbf{k}}\cdot\hat{\mathbf{r}}_{\alpha\beta}) \quad (3.11)$$

Equations (3.11) shows that the transfer function depends only on $\mathbf{r}_{\alpha\beta}$ which is the distance between the centers of non-adjacent (in far-field) groups. Moreover, if we move the source or target points (\mathbf{r}, \mathbf{r}') a small distance from their previous location (meaning another source and target points inside the same groups), the transfer function will not change and it computes the interaction between any two points close to the centers α and β .

Looking at eq.(3.10), we observe that computation of the sum of Green's functions evaluated between the target point \mathbf{r} and all the source points \mathbf{r}_n close to β can be easily performed, showing a fast computation of a matrix-vector product.

It shows that for each source location \mathbf{r}_n , we calculate the value of $e^{j\hat{\mathbf{k}}\cdot\mathbf{r}_n\beta}$ which from now we call it *radiation function*. Then these functions for all sources are aggregated to evaluate a local field at $\boldsymbol{\beta}$, the center of the segment. Then, this field is transmitted using transfer function to form a local field at $\boldsymbol{\alpha}$, the center of target points in a group. Multiplication of this local field with $e^{-j\hat{\mathbf{k}}\cdot\mathbf{r}_\alpha}$ (*receive function*) of the target point and the integration over unit sphere which we refer to as disaggregation, yields the desired summation.

In the next chapter where we modify our MOM solution to Hallen's integral equation, with SLFMM, you'll see how we locate our basis and test functions into the formulation of fast multipole algorithm to speed up MOM matrix-vector multiplication in order to find unknown current distribution on the thin wire dipole.

Chapter 4

Application of FMM on MOM

4.1 Reviewing the problem

Once more, we need to have a look at the thin wire antenna structure and formulations of Hallen's and Pocklington's integral equations in addition to the MOM solutions for both integral equations in order to modify them for FMM solution.

Consider the upper half-part of the wire shown in figure (4.1) with the length h oriented at the origin along z -axis. This cylindrical antenna is fed by DFG at the center (here the origin) by $V_i=1$ (volts). Therefore we can assume that voltage along the wire at any z_m point on the axis of the cylinder is one volt everywhere. Since the wire is very thin, we assume no current flow at the end points and consider only filamentary current on the surface of the cylinder (at z_n points) since the antenna is a good conductor.

Our moment method solution starts with discretization of the domain into $N-1$ segments (thus N observation and source points z_m and z_n ($n,m=1,2,\dots,N$) on the axis and surface respectively). Then approximating the current by the sum of weighted basis functions, which in case of Hallen's IE and $f(z') = \cos\left(\frac{n\pi z'}{h}\right)$

(entire-domain) basis function yields;

$$\int_0^h \sum_{n=1}^N \left(I_n \cos\left(\frac{n\pi z'}{h}\right) \right) \frac{e^{-jkR}}{4\pi R} dz' = -\frac{j}{\eta} [B \cos(kz) + C \sin(k|z|)] \quad (4.1)$$

and interchanging integral and summation goes to;

$$\sum_{n=1}^N I_n \int_0^h \cos\left(\frac{n\pi z'}{h}\right) \frac{e^{-jkR}}{4\pi R} dz' = -\frac{j}{\eta} [B \cos(kz) + C \sin(k|z|)] \quad (4.2)$$

where $R = \sqrt{(z-z')^2 + a^2}$. Inner product of both sides of eq.(4.2) with testing

functions $w(z) = \cos\left(\frac{m\pi z}{h}\right)$ ($m=1,2,\dots,N$), hence the name Galerkin method, we

have;

$$\sum_{n=1}^N I_n \int_0^h \cos\left(\frac{m\pi z}{h}\right) \int_0^h \cos\left(\frac{n\pi z'}{h}\right) \frac{e^{-jkR}}{4\pi R} dz' dz = \int_0^h -\frac{j}{\eta} \cos\left(\frac{m\pi z}{h}\right) [B \cos(kz) + C \sin(k|z|)] dz \quad (4.3)$$

Equation (4.3) can be transformed to the matrix equation $[Z][I]=[V]$ with unknown current coefficients I_n . Direct calculation of impedance matrix Z elements and inverting the matrix and even the matrix-vector multiplication of $[I]=[Z]^{-1}[V]$ is quite time and memory consuming process. Therefore we modify the solution of Hallen's IE by the fast multipole method algorithm in the next section.

for each row of matrices V and Z . This means that at each observation point, total source effect is the addition of effect of sources near to the observation point (in near field) and the effect of the far-field sources. For the sources in near-field of the observation point, we apply the regular matrix-vector multiplication resulted from Galerkin method and keep the values found for each observation point z_m , then we evaluate far field effects for that observation point and add it to the previous value to find the total effect in that specific target point.

4.3 Far-field Approximation

Let us start with grouping source points and target points as it is illustrated in figure (4.1) for SLFMM. Since we divide one arm into $N-1$ segment of height $\Delta z = \Delta z'$, we have $M=N$ target and source points.

Assumption 1: Let a (radius) to be very small ($a \ll 2h$) so we can put source points on the same axis of evaluation points, here z -axis ($\theta(\mathbf{r}, \mathbf{r}') \approx 0$).

we can form K groups each contains equal number (N/K) of source and target points namely β and α ($\alpha, \beta = 1, 2, \dots, K$) respectively according to figure (4.1) with group centers c_β, c_α .

Now, substituting equations (3.10) and (3.11) into the left hand side of eq.(4.3), writing the part which is forming our impedance matrix Z^{far} with interchanging the integral orders, we'll have;

$$Z_{mn}^{far} = \iint_1 T_L(k, \hat{\mathbf{k}}, \mathbf{r}_{\alpha\beta}) \int_0^h \cos\left(\frac{m\pi z}{h}\right) e^{-jk\hat{\mathbf{k}} \cdot \mathbf{r}_{m\alpha}} dz \int_0^h \cos\left(\frac{n\pi z'}{h}\right) e^{jk\hat{\mathbf{k}} \cdot \mathbf{r}'_{n\beta}} dz' \quad (4.5)$$

In the above equation, *assumption 1* help us to take all vectors along z-axis (even wave vector $\hat{\mathbf{k}} = \hat{a}_z$, since the problem reduced to a one dimensional problem). This and using the geometry of the problem we can write;

$$\mathbf{Z}^{far} = \begin{pmatrix} U_1 B_{11} W_1 & U_1 B_{12} W_2 & \cdots & U_1 B_{1K} W_K \\ U_2 B_{21} W_1 & & \ddots & \vdots \\ \vdots & & & \\ U_K B_{K1} W_1 & \cdots & & U_K B_{KK} W_K \end{pmatrix} \quad (4.6)$$

where for $\alpha, \beta = 1, 2, \dots, K$, $l, l' = 1, 2, \dots, L$ and $p, q = 1, 2, \dots, N/K$ we have;

$$\begin{aligned} [U_\alpha]_{pl} &= \int_{\left[\frac{p-1}{N} + \frac{\alpha-1}{K}, \frac{p}{N} + \frac{\alpha-1}{K}\right]} \cos\left(\frac{l\pi z}{h}\right) e^{-jk(z-c_\alpha)} dz \\ [W_\beta]_{l'q} &= \int_{\left[\frac{q-1}{N} + \frac{\beta-1}{K}, \frac{q}{N} + \frac{\beta-1}{K}\right]} \cos\left(\frac{l'\pi z'}{h}\right) e^{jk(z'-c_\beta)} dz' \\ [B_{\alpha\beta}]_{ll'} &= \begin{cases} T_l(k, \hat{a}_z, \mathbf{r}_{\alpha\beta}) & l = l' \text{ and } \alpha, \beta \text{ faraway} \\ 0 & \text{otherwise} \end{cases} \end{aligned} \quad (4.7)$$

where;

$$T_l(k, \hat{a}_z, \mathbf{r}_{\alpha\beta}) = \frac{k}{4\pi} \sum_{u=0}^l (-j)^{u+1} (2u+1) h_u^{(2)}(k|c_\alpha - c_\beta|)$$

because; $P_u(\hat{a}_z, \hat{\mathbf{r}}_{\alpha\beta}) = P_u(\cos \theta_{\alpha\beta}) = 1$ since $\theta_{\alpha\beta} = 0^\circ$ due to *assumption 1*.

Equation (4.6) can be rewritten as;

$$\mathbf{Z}^{far} = \begin{pmatrix} U_1 & 0 & \cdots & 0 \\ 0 & U_2 & \ddots & \vdots \\ \vdots & \ddots & \ddots & 0 \\ 0 & \cdots & & U_K \end{pmatrix} \begin{pmatrix} B_{11} & B_{12} & \cdots & B_{1K} \\ \vdots & & & \vdots \\ B_{K1} & B_{K2} & \cdots & B_{KK} \end{pmatrix} \begin{pmatrix} W_1 & 0 & \cdots & 0 \\ 0 & W_2 & \ddots & \vdots \\ \vdots & \ddots & \ddots & 0 \\ 0 & \cdots & & W_K \end{pmatrix} \quad (4.8)$$

or $Z^{far} = UBW$. Therefore, in the final steps of our moment method solution we will have;

$$[V] = [V^{near}] + [V^{far}] = [Z^{far}][I^{far}] + [Z^{near}][I^{near}]$$

while;

$$[V^{near}] = [Z^{near}][I^{near}] \Leftrightarrow [I^{near}] = [Z^{near}]^{-1}[V^{near}]$$

and

$$\begin{aligned} [V^{far}] = [Z^{far}][I^{far}] \Leftrightarrow [I^{far}] &= [Z^{far}]^{-1}[V^{far}] \\ &= [UBW]^{-1}[V^{far}] \\ &= [W]^{-1}[B]^{-1}[U]^{-1}[V^{far}] \end{aligned} \quad (4.9)$$

and finally; $[I] = [I^{near}] + [I^{far}]$.

Equation (4.9) shows how much SLFMM simplifies the solution of Hallen's IE for unknown current distribution, not only by means of reduction in the amount of memory needed, but speeds up the calculation of impedance matrix and its inverse (U and W matrices are block diagonal matrices which are easily inverted). Note that we should consider proper basis and test functions in eq.(4.7) when applying other moment methods for U and W in aggregation and disaggregation process.

It is to say that instead of computing matrix Z by calculation of order $O(N^2)$, matrices Z^{near} and Z^{far} are computed with lower order of computations. Matrix Z^{near} has nonzero entries in place of blocks $U_{\alpha}B_{\alpha\beta}W_{\beta}$ in eq.(4.6) where α, β are not faraway.

Under mild restrictions on the boundary (see [22],[8]), there are $O(K)$ of these blocks and each contains N^2 / K^2 entries. So the matrix Z^{near} has $O(N^2/K)$ nonzero entries. Each matrix U_α has Ln/K entries as does each W_β , while each $B_{\alpha\beta}$ has at most L nonzero entries. So, storage of Z^{near} and the decomposition of eq.(4.8) requires $O(N^2/K + LN + LK^2)$ storage locations which is smaller than $O(N^2)$ locations. We are free for choosing K in order to minimize complexity, but we should first find the value of L which is the length of expansion (truncation number) controlling the error of the approximation of or far-field matrix Z^{far} [22].

4.3.1 Number of Multipoles

In many books and papers, various amounts for L which is called the number of multipoles or truncation limit, is suggested. In [14] the suggested values for the number of multipoles are as follows;

- $L = kd + 5 \log(kd + \pi)$ (Rokhlin for single precision calculation)
- $L = kd + 10 \log(kd + \pi)$ (Rokhlin for double precision [14],[2])
- $L = kd + \beta(kd)^{1/3}$ (Chew and Song [14],[5])

where β is the number of digits of required accuracy ($\beta=6$ is sufficient for reasonable accuracy [14]) and d is the diameter (width) of each group.

Now, with everything in hand, once more we resolve Hallen's equation for unknown current on the thin wire antenna applying SLFMM on Galerkin method solution.

4.4 SLFMM Solution for Hallen IE

In this section, the same Hallen's IE we solved in section 2.3.2.1 will be resolved for unknown current density. The same entire-domain cosine function is considered as both basis and test functions (hence Galerkin).

We start again by dividing the domain (thin wire antenna upper arm) into $N-1=39$ segments, thus $N=40$ source points achieved. Considering equal number of evaluation points in the same coordination of source points and loop over each $p, q=8$ points makes a set of $K=5$ groups with 8 points for both source and targets with the width $d=h/K$ (h is the length of upper arm).

Then, by taking each two adjacent groups and applying the normal Galerkin method we compute the currents on each evaluation point due to the source points (here voltage points) which are in near field of that specific evaluation point. This will lead to 40 near basis function coefficients.

The next step is to find the same coefficients but this time, due to the sources which are faraway. To do so, first we'll find the group centers of each groups and directly form the matrices in eq.(4.8). using eq.(4.7). Note that the number of multipoles L is chosen due to the recommended one by *Chew* in 4.3.1 which rounded up to $L=5$. Therefore, we can form eq.(4.9) to compute currents on each target point due to its far basis functions.

Note that in eq.(4.7) the block matrices have the size as follows;

$$\text{Radiation Matrix: } W_{5 \times 5} = \begin{pmatrix} W_1 & 0 & \cdots & 0 \\ 0 & W_2 & \ddots & \vdots \\ \vdots & \ddots & \ddots & 0 \\ 0 & \cdots & & W_5 \end{pmatrix}$$

$$\text{Receive Matrix: } U_{5 \times 5} = \begin{pmatrix} U_1 & 0 & \cdots & 0 \\ 0 & U_2 & \ddots & \vdots \\ \vdots & \ddots & \ddots & 0 \\ 0 & \cdots & & U_5 \end{pmatrix}$$

$$\text{Transfer Matrix: } B_{5 \times 5} = \begin{pmatrix} B_{11} & B_{12} & \cdots & B_{15} \\ \vdots & & & \vdots \\ B_{51} & B_{52} & \cdots & B_{55} \end{pmatrix}$$

where the size for each block of W , U and B is;

$$[W_\beta]_{5 \times 8} \quad ; \quad [U_\alpha]_{8 \times 5} \quad ; \quad [B_{\alpha\beta}]_{5 \times 5 = L \times L} \quad (\alpha, \beta = 1, 2, \dots, K)$$

where each block in U is the conjugate transpose of the correspondent block in W .

Since U and V matrices are block diagonal, finding their inverse to form eq.(4.9) is easily performed by pseudo-inverting (inverse of non-square matrices $[W_\beta]_{5 \times 8}$ and $[U_\alpha]_{8 \times 5}$) each block elements of them to get another two block diagonal matrices U^{-1} and W^{-1} of the sizes 5×5 block-wise and 25×40 and 40×25 element-wise. To invert matrix B with the size of 25×25 (element-wise) we use less memory than inverting the original impedance matrix in direct MOM solution. Even by diagonalizing transfer matrix B , computation of its inverse can be performed faster and expansion of blocks may not be necessary.

Overall, equation (4.9) gives us the current distribution over the half-wire according to far field approximation and adding the near field and far field results for current we can find the overall current distribution illustrated in figure (4.2).

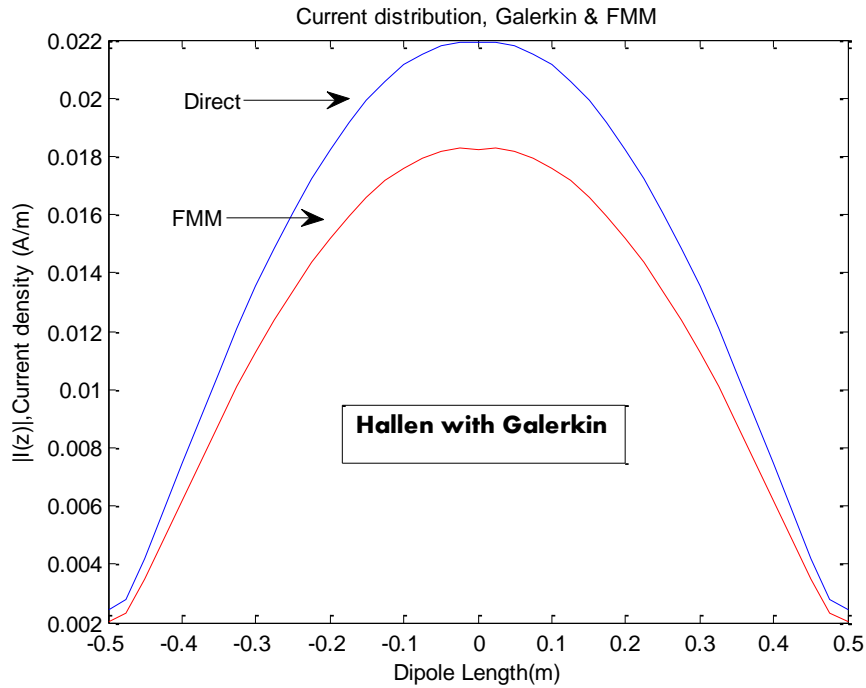


Figure 4.2: Current distribution for HE, over the thin wire, FMM

As it is shown in the figure above, the distribution computed by FMM is almost similar to the one in 2.3.2.1 for Hallen's IE with maximum 5.5% error at the center of the dipole. Similar to the direct Galerkin solution and boundary conditions at the end points are significantly satisfied.

Computational time using FMM is 15.582 seconds (12.821 seconds more than the computational time in direct method) but in terms of memory, the maximum memory allocation to form all near and far field matrix manipulations is about 10 KB which compared to the direct MOM (26.896 KB) shows a significant performance of applying FMM in this particular problem. Therefore, we can state that the fast

multipole method is a reliable technique for such problems, at least with the pre-defined assumptions for this particular integral equations in one dimension.

The results from solving n-body problems using FMM in different areas of science have shown that this method is quite useful and save time and memory which in problems with bigger and more complicated shape objects in 2D and 3D spaces, it shows its efficiency in terms of time and memory, especially when it comes to Multilevel Fast Multipole Method (MLFMM).

Chapter 5

CONCLUSION

To sum up the results of this thesis, we observe that in addition to applying moment method as an effective and strong numerical technique for solving Hallen and Pocklington's integral equations with point matching and Galerkin (comparing the results), combining the solution with Fast Multipole Method accelerates our solution and reduce the memory required for this particular numerical technique.

Although thin wire antenna problem and current distribution is not too much complicated when compared to 2D and 3D problems and may not have many applications in real life, performing FMM and MOM for this problem in this thesis at least give us the idea of how such fast algorithm can save time and memory when it comes to bigger and much more complicated antenna problems.

This algorithm and expanding the solution into 2D and 3D problems may be quite useful especially for bigger and more complicated objects which can be considered as the future work for this thesis.

Using such numerical techniques in reverse engineering can be performed for designing antennas with desired functionalities due to the desired distribution of the current which comes through the incoming or outgoing radiations.

REFERENCES

- [1] Balanis, C. A. (2005). *Antenna Theory Analysis and Design* (Third Edition ed.). New Jersey: John Wiley & Sons, Inc.
- [2] Balanis, C. A. (2008). *Modern Antenna Handbook*. United States of America, Canada: John Wiley & Sons, Inc.
- [3] Butler, D. R. (1975). *On Some Simple, Numerically Efficient Techniques for Handling Electric-Field Integral Equations (Lecture Note 218)*. Mississippi: University of Mississippi.
- [4] Chew, W. C., Jin, J. M., & Song, E. M. (2001). *Fast and Efficient Algorithms in Computational Electromagnetics*. Massachusetts, USA: Hard Cover.
- [5] Crosswell, C.W.(1990, June). Origin and Development of the Method of Moments for field Computation. *IEEE Antennas and Propagation Society Magazine*
- [6] D. H. Werner, P. L. (1994, April). Some Computational Aspects of Pocklington's Electric Field Integral Equation for Thin Wires. *IEEE Transactions on Antennas and Propagation*, 42(4), 561-563.
- [7] Darve, E. (2000). The Fast Multipole Method: Numerical Implementation. *Journal of Computational Physics*(No.160), 195-240.
- [8] Darve, E. (2001). Efficient Fast Multipole Method for low frequency scattering. *Center for Turbulence Research*, 259-271.

- [9] Davidson, D. B. (2005). *Computational Electromagnetics for RF and Microwave Engineering*. (S. A. Department of Electrical and Electronic Engineering University of Stellenbosch, Ed.) Cambridge, Uk: Cambridge University Press.
- [10] Duraiswami, N. A. (2005, April 12). Comparison of the efficiency of translation operators used in the fast multipole method for the 3D Laplace equation. *Gumerov & Duraiswami*, University of Maryland, CS TR 4701, UMIACS TR.1-43.
- [11] Engblom, S. (2011, Aug 10). On well-separated sets and fast multipole methods. *Elsevier*, 1-8.
- [12] Fikioris, G. (2011). On The Solvability and Application Of Numerical Methods To Hallen's Equation. (D. o. Athens, Ed.) *MMET*, 73-79.
- [13] Fikioris, G., & Wu, T. T. (2001, March). On the Application of Numerical Methods to Hallén's Equation. *IEEE Transactions on Antennas and Propagation*, 40(No.3), 383-393.
- [14] Gibson, W. C. (2008). *The Method of Moments in Electromagnetics*. New York, USA: Taylor & Francis Group.
- [15] Giri, D. V., & Baum, B. K. (1975). *Accurate Evaluation of the Impedance Matrix Elements in the Hallen Integral Equation for Wire Antennas (Lecture Note 40)*. USA: Air Force Weapons Laboratory.
- [16] Greengard, R. B. (2009). A short course on fast multipole methods. Courant Institute of Mathematical Sciences, , Department of Mathematics and Statistics,, New York: New York University,University of Canterbury.

- [17] Harrington, R. F. (1992). *Field Computation by Moment Methods*. (S. University, Ed.) New York, USA: IEEE Press.
- [18] Jiming Song, C.-C. L. (1997, October). Multilevel Fast Multipole Algorithm for Electromagnetic Scattering by Large Complex Objects. *IEEE Transactions on Antennas and Propagation*, 45(No.10), 1488-1494.
- [19] Kalyan C. Donepudi, J. S. (2000, August). A Novel Implementation of Multilevel Fast Multipole Algorithm for Higher Order Galerkin's Method. *IEEE Transactions on Antennas and Propagation*, 48(No.8), 1192-1196.
- [20] Marasini, C. (2008). *Efficient computation techniques for Galerkin MOM antenna design*. Lucca, Italy: Technische Universiteit Eindhoven.
- [21] Michalopoulou, G. F. (2009). On the Use of Entire-Domain Basis Functions in Galerkin Methods Applied to Certain Integral Equations for Wire Antennas With the Approximate Kernel. *IEEE Transactions on Electromagnetic Compatibility*, 51(No.2), 409-413.
- [22] Profit, S. A. (2009). *Analysis of Diagonal Form of The Fast Multipole Algorithm For Scattering Theory*. Department of Computer and Mathematical Sciences. England: University of Salford.
- [23] Rokhlin, N. Y. (1997, January). *An Improved Multipole Algorithm for Potential Fields On One-Dimensional Structures*. USA: Research Report YALEU.
- [24] Rokhlin, N. Y. (1998). *A Generalized One-Dimensional Fast Multipole Method with Application to Filtering of Spherical Harmonics*. USA: Research Report YALEU.

- [25] Rokhlin, N. Y. (1999). An Improved Fast Multipole Algorithm for Potential Fields on the Line. *SIAM Journal on Numerical Analysis* , 36(No.2), 629-666.
- [26] Rokhlin, P. G. (2007). An Accelerated Kernel-Independent Fast Multipole Method. *Society for Industrial and Applied Mathematics*, 29(3), 1160-1178.
- [27] Rokhlin, P. G. (2007). An Accelerated Kernel-Independent Fast Multipole Method in One Dimension. *SIAM J.*, 29(No.3), 1160-1178.
- [28] Sadiku, N.M. (2001). *Numerical techniques in Electromagnetics*. (2nd Ed.). Boca Raton, Florida: CRC Press LLC.
- [29] Sarkar, T. K. (1981). *A Study of the Various Methods for Computing Electromagnetic Fields Utilizing Thin Wire Integral Equations (Lecture Note 422)*. New York: Department of Electrical Engineering Rochester Institute of Technology.
- [30] Sertel, J. L. (2012). *Integral Equation Methods for Electromagnetics*. The Ohio State University: SciTech Publishing Inc.
- [31] Steinbach, O., & Wendland, W. L. (2004). The fast multipole method for the symmetric boundary integral formulation. *IMA Journal of Numerical Analysis*.,26(No.2), 272-296.
- [32] Sun, X., & Pitsianis, N. P. (2001). A Matrix Version of the Fast Multipole Method. (S. f. Mathematics, Ed.) *SIAM REVIEW*, 43(No.2), 289-300.
- [33] Tosun, H. (2008). *Numerical methods in Electromagnetic. (Lecture notes)*. Famagusta. Turkish Republic of North Cyprus: Eastern Mediterranean University.

- [34] Warnick, K. F. (2008). *Numerical Analysis for Electromagnetic Integral Equations*. Norwood, MA, USA: Artech House, Inc.
- [35] Warnick, K. F. (2011). *Numerical Methods for Engineering (An Introduction Using MATLAB nad Computational Electromagnetics Examples)*. Raleigh: SciTech Publishing Inc.
- [36] Zhibin Zhao, J. L. (2008). The Fast Multipole Method for Analysis of Electromagnetic Scattering from Thin-wire Antennas. *North China Electric Power University*, 2-5.

APPENDICES

Appendix A: Matlab Programs for Point Matching MOM

A-1: Hallen's integral Equation

```
%------%
%------%
%-----Matlab code for figure(2.7)where L=lamda/2------%
%-----and figure(2.8)where L=1.5Lamda------%
%------%
clc
clear all
clc
%----- Constants ----- %
c=3.0e+08;
etha=377;
Frequency=1.5e+08; %Operating Frequency%
Voltage=1; %Applied Voltage%
lamda=c/Frequency; %Wavelength of the field%
L=lamda/2; %Length of the Wire%
a=L/518; %Radius of the Wire%
k=2*pi/lamda;
N=40; %Number of Segments%
delta=L/(N);
%----- %
t=linspace (-0.5*L,0.5*L,N);
zm=-0.5*L-delta
for m=1:N+1
    zm=zm+delta;
    zn=-0.5*L+delta/2;
    for n=1:N+1
        if (n==N+1)
            A(m,n)=-i*cos(k*zm)/(etha);
        else
            syms z
            R=sqrt(a^2+(z-zm)^2);
            g=inline([exp(-i*k*R)/(4*pi*R)]);
            G=quad(g,zn,zn+delta/2);
            A(m,n)=G;
        end
        zn=zn+delta;
    end
    V(m,1)=[-i*Voltage*sin(k*abs(zm))]/(2*etha);
end
Ainv=inv(A);
I=(Ainv*V);
for p=1:N
    P(p,1)=I(p,1);
end
plot(t,abs(P),t,real(P),'g',t,imag(P),'r')
xlabel('Dipole Length (m)')
ylabel('I(z),Current density (A/m)')
title('Current distribution over dipole antenna f=150 MHz')
```

A-2: Hallen vs. Pocklington

```

%-----%
%-----%
%-----Matlab code for figure(2.9)-----%
%-----%
%-----%

clear all
clc
%-----Costants-----%
c=3.0e+08;
etha=377;
Frequency=3.0e+08;    %Operating Frequency%
Voltage=1;            %Applied Voltage%
lamda=c/Frequency;   %Wavelength of the Field%
L=0.47*lamda;        %Length of the Wire%
a=0.005*lamda;       %Radius of the Wire%
k=2*pi/lamda;
N=21;                %Number of Segments%
delta=L/(N);
%-----%

t=linspace (-0.5*L,0.5*L,N);
zm=-0.5*L-delta;
for m=1:N+1
    zm=zm+delta;
    zn=-0.5*L+delta/2;
    for n=1:N+1
        if (n==N+1)
            A(m,n)=-cos(k*zm);
        else
            syms z
            R=sqrt(a^2+(z-zm)^2);
            g=inline([exp(-i*k*R)/(4*pi*R)]);
            G=quad(g,zn,zn+delta/2);
            A(m,n)=G;
        end
        zn=zn+delta;
    end
    V(m,1)=[-i*Voltage*sin(k*abs(zm))]/(2*etha);
end
Ainv=inv(A);
I=(Ainv*V);
for h=1:N
    H(h,1)=I(h,1);
end
zm=-0.5*L-delta;
for m=1:N+1
    zm=zm+delta;
    zn=-0.5*L+delta/2;
    for n=1:N+1
        if (n==N+1)
            A(m,n)=-i*cos(k*zm)/(etha);
        else
            syms z
            R=sqrt(a^2+(z-zm)^2);
            g=inline([exp(-i*k*R)/(4*pi*R^5)]*[ (1+j*k*R)*(2*R^2-
3*a^2)+(k*a*R)^2]);
            G=quad(g,zn,zn+delta);
            A(m,n)=-lamda*etha*G/(8*pi^2*i);
        end
        zn=zn+delta;
    end
end

```

```

    end
    V(m,1)=[-i*Voltage*sin(k*abs(zm))]/(2*etha);
end
Ainv=inv(A);
I=(Ainv*V);
for p=1:N
    P(p,1)=I(p,1);
end
plot(t,abs(H)/abs(max(H)),t,abs(P)/abs(max(P)),'r')
xlabel('Dipole Length (m)')
ylabel('I(z),Current density (A/m)')
title('Current distribution, Hallen Vs. Pocklington')

```

Appendix B: Matlab Programs for Galerkin MOM

B-1: Hallen's Integral Equation ($a=L/518$)

```

%-----This Matlab code computes current distribution-----%
%-----for HE,using Galerkin method with entire domain-----%
%-----basis and test functions-----%
%-----The result is shown in figure(2.10) with the result of-----%
%-----the code in appendix A-1 for comparison-----%
%-----%
clear all
clc
%-----Costants-----%
c=3.0e+08;
etha=377;
Frequency=1.5e+08;    %Operating Frequency%
Voltage=1;            %Applied Voltage%
lamda=c/Frequency;   %Wavelength of the Field%
L=lamda/2;           %Length of the Wire%
a=L/518;             %Radius of the Wire%
k=2*pi/lamda;
N=40;               %Number of Segments%
delta=L/(N);
h=L/2;
for m=1:N+1
    for n=1:N+1;
        G2=0;
        for z=-h:delta:h
            G1=0;
            for zp=-h:delta:h
                R=sqrt(a^2+(z-zp)^2);
                g1=(exp(-1i*k*R)/(4*pi*R))*cos(n*pi*zp/L)*delta;
                G1=g1+G1;
            end
            g2=cos(m*pi*z/L)*delta*G1;
            G2=g2+G2;
        end
        A(m,n)=G2;
    end
end
z=-h:delta:h;
vm1=-(0.5i*delta/etha)*cos(m*pi*z/L).*sin(k*abs(z));
vm2=-delta*cos(m*pi*z/L).*cos(k*z);
V1(m,1)=sum(vm1);
V2(m,1)=sum(vm2);
end
I1=A\V1;
I2=A\V2;
n=0:N;
nom=(-1).^n.*I1';
denom=(-1).^n.*I2';
C=sum(nom)/sum(denom);
In=(I1+C*I2)
m=0;
for z=-h:delta:h;
    m=m+1;
    I(m,1)=0;
    for n=1:41

```

```

        Iz=In(n)*cos(n*pi*z/L);
        I(m,1)=I(m,1)+Iz;
    end
end
t=-h:delta:h;
plot(t,abs(I))
xlabel('Dipole Length (m)')
ylabel('I(z),Current density (A/m)')
title('Current distribution over dipole antenna f=150 MHz')

```

B-2: Hallen's Integral Equation ($a=0.01\lambda$)

```

%-----%
%-----%
%-----Matlab code for figures (2.11), (2.12), (2.13), (2.14)-----%
%-----%
%-----%
clear all
clc
%-----Costants-----%
c=3.0e+08;
etha=377;
Frequency=1.5e+08;    %Operating Frequency%
Voltage=1;            %Applied Voltage%
lamda=c/Frequency;   %Wavelength of the Field%
L=lamda/2;           %Length of the Wire%
a=0.01*lamda;        %Radius of the Wire%
k=2*pi/lamda;
N=40;                %Number of Segments%
h=L/2;
dz=h/N;dzp=h/N;
for m=1:N+1
    for n=1:N+1;
        G2=0;
        for z=dz:dz:h+dz
            G1=0;
            for zp=0:dzp:h
                R=sqrt(a^2+(z-zp)^2);
                RP=sqrt(a^2+(z+zp)^2);
                g1=((exp(-1i*k*R)/(4*pi*R))+exp(-
1i*k*RP)/(4*pi*RP))*cos((n-1)*pi*zp/h)*dzp;
                G1=g1+G1;
            end
            g2=cos((m-1)*pi*z/h)*dz*G1;
            G2=g2+G2;
        end
        A(m,n)=G2;
    end
end
z=dz:dz:h+dz;
vm1=(0.5i/etha)*cos((m-1)*pi*z/h).*sin(k*z)*dz;
vm2=cos((m-1)*pi*z/h).*cos(k*z)*dz;
V1(m,1)=sum(vm1);
V2(m,1)=sum(vm2);
end
I1=A\V1;
I2=A\V2;
n=0:N;
nom=(-1).^n.*I1';
denom=(-1).^n.*I2';

```

```

C=sum(nom)/sum(denom);
In=(I1+C*I2)
z=0:dz:h;
z=z';
nz=z*n;
Iz=In'*cos((pi/h)*nz);
zl=0:-dz:-h;
zr=0:dz:h;
subplot(2,2,1)
plot(zl/lamda,real(Iz),zr/lamda,real(Iz),'b')
xlabel('z/lamda (m)')
ylabel('Re {I(z)},Current density (A/m)')
title('Current distribution, Hallen ')
subplot(2,2,2)
plot(zl/lamda,imag(Iz),zr/lamda,imag(Iz),'b')
xlabel('z/lamda (m)')
ylabel('Img {I(z)},Current density (A/m)')
title('Current distribution, Hallen ')
n=0:N;
subplot(2,2,3)
plot(n,real(In))
xlabel('n')
ylabel('Re {I(n)},Basis function coefficients')
title('Current distribution, Hallen ')
subplot(2,2,4)
plot(n,imag(In))
xlabel('n')
ylabel('Img {I(n)},Basis function coefficients')
title('Current distribution, Hallen ')
figure()
subplot(1,2,1)
plot(zl/lamda,abs(Iz),zr/lamda,abs(Iz),'b')
xlabel('z/lamda (m)')
ylabel('Magnitude {I(z)},Current density (A/m)')
title('Current distribution, Hallen ')
subplot(1,2,2)
plot(n,abs(In))
xlabel('n')
ylabel('Magnitude {I(n)},Basis function coefficients')
title('Current distribution, Hallen ')

```

B-3: Pocklington's Integral Equation

```

%-----%
%-----This Matlab code computes current distribution-----%
%-----for PE,using Galerkin method with entire domain-----%
%-----basis and test functions-----%
%-----%
%-----The result is shown in figure(2.15) with the result of-----%
%-----the code in appendix A-2 for comparison-----%
%-----%
clear all
clc
%-----Costants-----%
c=3.0e+08;
etha=377;
Frequency=1.5e+08;    %Operating Frequency%

```

```

Voltage=1;           %Applied Voltage%
lamda=c/Frequency;  %Wavelength of the Field%
L=lamda/2;          %Length of the Wire%
a=L/518;            %Radius of the Wire%
k=2*pi/lamda;
N=40;               %Number of Segments%
delta=L/(N);
h=L/2;

for m=1:N+1
    for n=1:N+1;
        G2=0;
        for z=-h:delta:h
            G1=0;
            for zp=-h:delta:h
                R=sqrt(a^2+(z-zp)^2);
                g1=(exp(-1i*k*R)/(4*pi*R^5))*((1+i*k*R)*(2*R^2-
3*a^2)+(k*a*R)^2)*cos(n*pi*zp/h)*delta;
                G1=g1+G1;
            end
            g2=cos(m*pi*z/h)*delta*G1;
            G2=g2+G2;
        end
        A(m,n)=G2;
    end
end
z=-h:delta:h;
vm1=-(0.5i*delta/etha)*cos(m*pi*z/h).*sin(k*abs(z));
vm2=-delta*cos(m*pi*z/h).*cos(k*z);
V1(m,1)=sum(vm1);
V2(m,1)=sum(vm2);
end
I1=A\V1;
I2=A\V2;
n=0:N;
nom=(-1).^n.*I1';
denom=(-1).^n.*I2';
C=sum(nom)/sum(denom);
In=(I1+C*I2)
m=0;
for z=-h:delta:h;
    m=m+1;
    I(m,1)=0;
    for n=1:41
        Iz=In(n)*cos(n*pi*z/h);
        I(m,1)=I(m,1)+Iz;
    end
end
end
t=-h:delta:h;
plot(t,abs(I)/0.002)
xlabel('Dipole Length (m)')
ylabel('I(z),Current density (A/m)')
title('Current distribution over dipole antenna f=150 MHz')

```


Appendix C: Matlab Program for FMM and Galerkin Method(HE)

```

%-----%
%-----%
%-----This Matlab code,computes the current distribution-----%
%-----over the wire antenna for Hallen's integral equation-----%
%-----modifying Galerkin method with FMM-----%
%-----Results of this code and the code in Appendix B-1 has-----%
%-----been illustrated in figure (4.2)-----%
%-----%

clear all
clc
%-----Costants-----%
c=3.0e+08;
etha=377;
Frequency=1.5e+08;    %Operating Frequency%
Voltage=1;            %Applied Voltage%
lamda=c/Frequency;    %Wavelength of the Field%
Length=lamda/2;       %Length of the Wire%
radius=Length/518;    %Radius of the Wire%
k=2*pi/lamda;
N=40;                 %Number of points%
delta=Length/(N-1);
L=5;                 %mnumber= number of multipoles  L=kd+beta*(kd)^(1/3)
beta=6,d=group width
K=5;                 %Number of groups%
a=1:K;b=1:K;         %Group numbers
l=1:L;lp=1:L;
P=N/K;Q=N/K;         %number of target/source points in each group
%-----Near Field Calculations-----%
h=P*delta;          %width of segments
H=2*h;
INear=zeros(N,1);
for t=0:K-2
    for m=1:2*P
        for n=1:2*Q
            G2=0;
            for z=-h:delta:h
                G1=0;
                for zp=-h:delta:h
                    R=sqrt(radius^2+(z-zp)^2);
                    g1=(exp(-1i*k*R)/(4*pi*R))*cos(n*pi*zp/H)*delta;
                    G1=g1+G1;
                end
                g2=cos(m*pi*z/H)*delta*G1;
                G2=g2+G2;
            end
            A(m,n)=G2;
        end
        z=-h:delta:h;
        vm1=(-0.5i/etha)*cos(m*pi*z/H).*sin(k*abs(z))*delta;
        vm2=cos(m*pi*z/H).*cos(k*z)*delta;
        V1(m,1)=sum(vm1);
        V2(m,1)=sum(vm2);
    end
end
I1=A\V1;
I2=A\V2;
n=0:2*P-1;
nom=(-1).^n.*I1';
denom=(-1).^n.*I2';

```

```

C=sum(nom)/sum(denom);
In=(I1+C*I2);
if t==0
    INear=[In;zeros(N-(t+2)*P,1)];
else

INear=[INear(1:t*P);INear(t*P+1:(t+1)*P)+In(1:P);In(P+1:2*P);zeros(N
-(t+2)*P,1)];
end
end
%-----Far Field Calculations-----%

ca=(P-1)*delta/2:h:Length-(P-1)*delta/2; %group centers
cb=(Q-1)*delta/2:h:Length-(Q-1)*delta/2;

%-----Receive and Radiation Matrices-----%
for b=1:K
    for lp=1:L
        for q=1:Q
            syms zp
            Rad=inline(exp(1i*k*(zp-cb(b)))*cos(lp*pi*zp/h));
            W(lp,q,b)=quad(Rad,Length*((q-1)/(N-1)+(b-
1)/K),Length*(q/(N-1)+(b-1)/K));
        end
    end
end
RAD=blkdiag(W(:,:,1),W(:,:,2),W(:,:,3),W(:,:,4),W(:,:,5));
for a=1:K
    for p=1:P
        for l=1:L
            syms z
            Rcv=inline(exp(-1i*k*(z-ca(a)))*cos(l*pi*z/h));
            U(p,l,a)=quad(Rcv,Length*((p-1)/(N-1)+(a-
1)/K),Length*(p/(N-1)+(a-1)/K));
        end
    end
end
RCV=blkdiag(U(:,:,1),U(:,:,2),U(:,:,3),U(:,:,4),U(:,:,5));
%-----Transfer Matrix-----%

for a=1:K
    for b=1:K
        for l=1:L
            for lp=1:L
                if (abs(a-b) > 1) & (l==lp)
                    t=0:l;
                    T=(-
1i).^ (t+1) .* (2*t+1) .*besselh(t,2,k*abs(ca(a)-cb(b)));
                    B(l,lp,a,b)=k*sum(T)/(4*pi);
                else
                    B(l,lp,a,b)=0;
                end
            end
        end
    end
end
end
B2D=zeros(K*K,K*K);

```

```

for xm=1:K:K^2-K+1
    xM=xm+(K-1);
    for ym=1:K:K^2-K+1
        yM=ym+(K-1);
        B2D(xm:xM,ym:yM)=B(:, :, xM/K, yM/K);
    end
end
AF=pinv(RAD)*(B2D\pinv(RCV));
for m=1:N
    z=-Length/2:delta:Length/2;
    vm1=-(0.5i/etha)*cos(m*pi*z/Length).*sin(k*z)*delta;
    vm2=cos(m*pi*z/h).*cos(k*z)*delta;
    V1(m,1)=sum(vm1);
    V2(m,1)=sum(vm2);
end
I1=AF*V1;
I2=AF*V2;
n=0:N-1;
nom=(-1).^n.*I1';
denom=(-1).^n.*I2';
C=sum(nom)/sum(denom);
IF=(I1+C*I2);
IF=I2+I1;
InTotal=IF+INear;
m=0;
for z=-Length/2:delta:Length/2;
    m=m+1;
    I(m,1)=0;
    for n=1:40
        Iz=InTotal(n)*cos(n*pi*z/Length);
        I(m,1)=I(m,1)+Iz;
    end
end
end
z=-Length/2:delta:Length/2;
plot(z,I)
xlabel('Dipole Length(m)');
ylabel('|I(z)|,Current density (A/m)')
title('Current distribution, Galerkin & FMM')

```